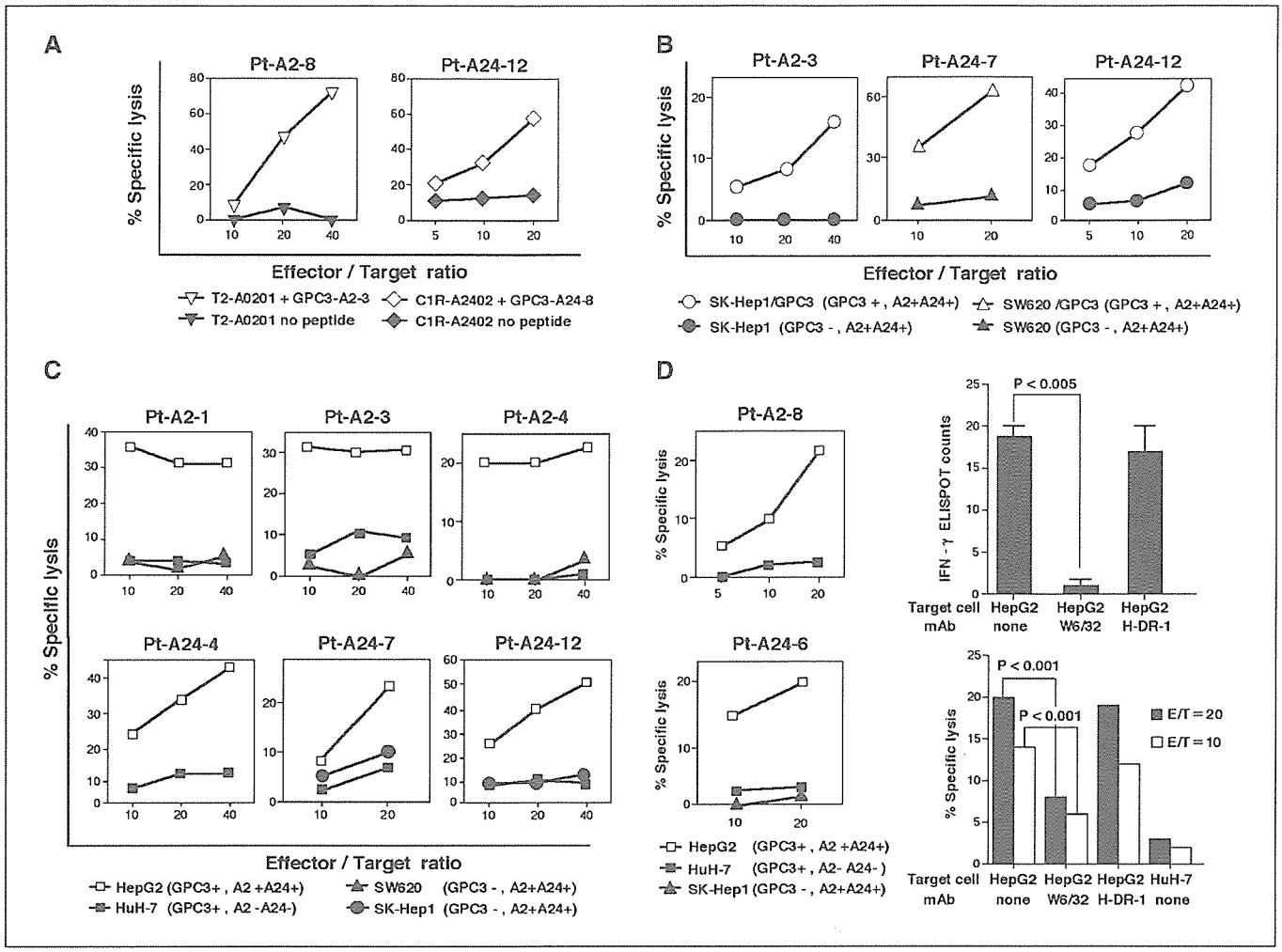

Fig. 3. CTL induction from PBMCs of HLA-A2- or HLA-A24-positive HCC patients. *A* and *B*, GPC3 peptide-reactive CTLs were generated from $CD8^+$ T cells of $HLA\text{-}A2^+$ and/or $HLA\text{-}A24^+$ HCC patients. After three or four stimulations with autologous monocyte-derived DCs pulsed with the $GPC3_{144\text{-}152}$ or $GPC3_{298\text{-}306}$ peptide, the CTLs were subjected to a standard ^{51}Cr release assay at the indicated effector/target ratio. Their cytotoxicity against the $GPC3_{298\text{-}306}$ peptide pulsed C1R-A2402 cells or T2-A0201 cells, and each unpulsed cells (*A*), or $GPC3^-$ $HLA\text{-}A2^+$, $HLA\text{-}A24^+$ HCC cell line SK-Hep-1, $GPC3^-$ $HLA\text{-}A2^+$, $HLA\text{-}A24^+$ colon cancer cell line SW620, and those cell lines transfected with the human *GPC3* gene; SK-Hep-1/GPC3 or SW620/GPC3 (*B*) were examined by a ^{51}Cr release assay. *C* and *D*, $GPC3^+$ $HLA\text{-}A2^+$, $HLA\text{-}A24^+$ HCC cell line HepG2, $GPC3^+$ $HLA\text{-}A2^-$, $HLA\text{-}A24^-$ HCC cell line HuH-7, and $GPC3^-$ tumor cell lines SW620 and SK-Hep1 were used as target cells (*left*). *Points,* percentage of specific lysis calculated based on the mean values of a triplicate assay. *D*, inhibition of cytotoxicity by anti-HLA class I mAb (*right*). After the target HepG2 cells were incubated with anti-HLA class I mAb (W6/32, IgG_{2a}) or anti-HLA DR mAb (H-DR-1, IgG_{2a}), respectively, for 1 hour, the CTLs generated from PBMCs of patient A2-8 by stimulation with $GPC3_{144\text{-}152}$ peptide (*top*) or CTLs generated from patient A24-6 using the $GPC3_{298\text{-}306}$ peptide (*bottom*) were added. IFN-γ production (*top*; IFN-γ ELISPOT assay) and cytotoxicity (*bottom*; ^{51}Cr release assay) were markedly inhibited by W6/32, but not by H-DR-1.

HLA-A24+), but not to HuH-7 (GPC3+, HLA-A2−, and HLA-A24−) or SW620 ($GPC3^-$, HLA-A2+, and HLA-A24+) in patients A2-1, A2-3, and A2-4. Similarly, we could generate GPC3-reactive CTLs by stimulation of PBMCs with the $GPC3_{298\text{-}306}$ peptide and these CTLs exhibited cytotoxic activity to HepG2, but not to HuH-7 or SK-Hep-1 ($GPC3^-$, HLA-A2+, HLA-A24+) in patients A24-4, A24-7, and A24-12.

In an HLA-class I blocking experiment, anti-HLA class I mAb W6/32 markedly inhibited the IFN-γ production stimulated with HepG2 cells in ELISPOT assay of CTLs generated from patient A2-8 by stimulation with the $GPC3_{144\text{-}152}$ peptide (Fig. 3D, top), and inhibited cytotoxic activity against HepG2 cells in ^{51}Cr release assay of CTLs generated from patient A24-6 by stimulation with the $GPC3_{298\text{-}306}$ peptide (Fig. 3D, bottom), but anti-HLA-DR mAb, H-DR-1 did not inhibit the response of CTLs. These results clearly indicate that these CTLs recognized HepG2 in a HLA-class I–restricted manner.

As shown in Table 2, we could induce GPC3-reactive CTLs from PBMCs in ~50% of either the HLA-A2− or HLA-A24-positive HCC patients. In patients A2-6, A24-5, A24-9, and A24-11 who did not express GPC3 in tumor tissues, GPC3-reactive CTLs could not be induced from their PBMCs. Among eight HLA-A2-positive HCC patients who expressed GPC3 in HCC tissue or produced soluble GPC3 in sera, patients A2-1, A2-2, A2-3, A2-4, A2-6, A2-7, A2-9, and A2-10, GPC3-reactive CTLs could be generated from the PBMCs of only four patients (50%). In patient A2-6, GPC3 was detected only in the serum but not in HCC tumor tissue. It was thought to be possible that the majority of GPC3 protein was secreted away in this type of HCC cell as described previously (7). Among six HLA-A24-positive patients who expressed GPC3 in tumor tissue, patients A24-1, A24-2, A24-3, A24-6, A24-10, and A24-12, GPC3-reactive CTLs could be generated from the PBMCs of only four patients (67%). We also examined whether it was possible to

induce GPC3-specific CTLs from PBMCs isolated from healthy donors (each HLA type, $n = 3$), but we failed to generate GPC3-specific and HLA-A2- or HLA-A24-restricted CTLs even though PBMCs were stimulated with the peptides thrice *in vitro* (data not shown). These results suggest that GPC3-reactive CTLs could only be induced in patients who expressed GPC3 in tumor tissue, thus, indicating the existence of GPC3-reactive CTL precursors in patients with GPC3$^+$ HCC. We also examined whether GPC3-reactive CTLs could be generated more frequently from PBMCs isolated from HCC patients positive for serum-soluble GPC3. As shown in Table 2, the presence of serum-soluble GPC3 did not correlate statistically with the successful induction of GPC3-reactive CTLs. As a result, we could not observe the enhancement of CTL induction efficiency via possible antigen presentation of soluble serum GPC3 through HLA-class II pathways to CD4$^+$ T cells or cross-presentation through the HLA class I pathway to CD8$^+$ T cells (25, 26) in patients positive for serum GPC3.

Inoculation of the GPC3 peptide-induced CTLs reduced growth of a GPC3$^+$ human HCC tumor cell line implanted into NOD/SCID mouse. To investigate the effects of GPC3 peptide-reactive CTL inoculation into the mice implanted with the GPC3$^+$ human HCC cell line, we s.c. inoculated SK-Hep1/GPC3 cell lines positive for both HLA-A2 and HLA-A24 into NOD/SCID mice, and i.v. injected the mixture of CTLs generated from several HCC patients positive for HLA-A2 or HLA-A24 into mice implanted with SK-Hep1/GPC3 when the diameter of these tumors reached 5 × 5 mm in size as described in Materials and Methods. The CTLs injected into mice were prepared by stimulating peripheral blood CD8$^+$ T cells with HLA-A2- or HLA-A24-restricted GPC3-epitope peptides or control-irrelevant HIV peptides as described in Materials and Methods. The tumor sizes of four individual mice in each group (Fig. 4A) and mean ± SD of tumor sizes in each group (Fig. 4B) were evaluated. After 5 days from the second inoculation of GPC3 peptide-reactive CTLs, the tumor size of SK-Hep1/GPC3 was apparently reduced in comparison to the size of tumor mass implanted into NOD/SCID mice injected with control T cells or saline alone ($P < 0.01$). These results clearly indicate the efficacy of adoptive GPC3 peptide-reactive CTL transfer therapy for GPC3$^+$ tumor in mice.

Discussion

In this article, we identified HLA-A24-restricted or HLA-A2-restricted GPC3 CTL epitope peptides, and found that

Table 2. Expression of GPC3 in HCC tissue, quantification of serum-soluble GPC3, and GPC3-specific CTL induction in HCC patients

	Age	Gender	State of tumor*	GPC3 expression†	Serum GPC3‡	HLA expression§	CTL induction‖
HLA-A2 (*A*0201*) – positive patients							
Pt-A2-1	80	F	IIIa	+	+	+	+
Pt-A2-2	72	M	II	+	+	+	+
Pt-A2-3	67	F	II	ND	+	ND	+
Pt-A2-4	54	M	I	+	–	+	+
Pt-A2-5	57	M	I	ND	–	ND	–
Pt-A2-6	66	M	I	–	+	–	–
Pt-A2-7	54	M	IIIa	+	–	+	–
Pt-A2-8	73	M	II	ND	–	ND	+
Pt-A2-9	68	F	IIIa	+	–	+	–
Pt-A2-10	54	M	II	+	+	+	–
HLA-A24 (*A*2402*)-positive patients							
Pt-A24-1	60	M	IVa	+	+	+	+
Pt-A24-2	57	M	IVa	+	+	+	–
Pt-A24-3	75	F	IIIa	+	+	+	+
Pt-A24-4	59	M	IIIa	ND	–	ND	+
Pt-A24-5	52	M	IVb	–	–	+	–
Pt-A24-6	65	M	I	ND	+	ND	+
Pt-A24-7	61	M	I	ND	–	ND	+
Pt-A24-8	74	M	II	ND	–	ND	–
Pt-A24-9	59	M	IVb	–	–	–	–
Pt-A24-10	69	M	IVa	+	+	+	–
Pt-A24-11	72	M	II	–	–	+	–
Pt-A24-12	61	M	IIIa	+	+	+	+

Abbreviations: F, female; M, male; ND, not determined.
*Tumor-node-metastasis classification.
†Positive (+) or negative (–) staining of tumor cells in contrast with peritumor normal tissue as background staining.
‡Serum levels >106 ng/mL were evaluated as positive.
§Immunohistochemical staining of the membrane of tumor cells was evaluated as positive.
‖Specific lytic activity (≧20%) at E:Tratio = 20 against HepG2 target cells was evaluated as positive by ^{51}Cr release assay.

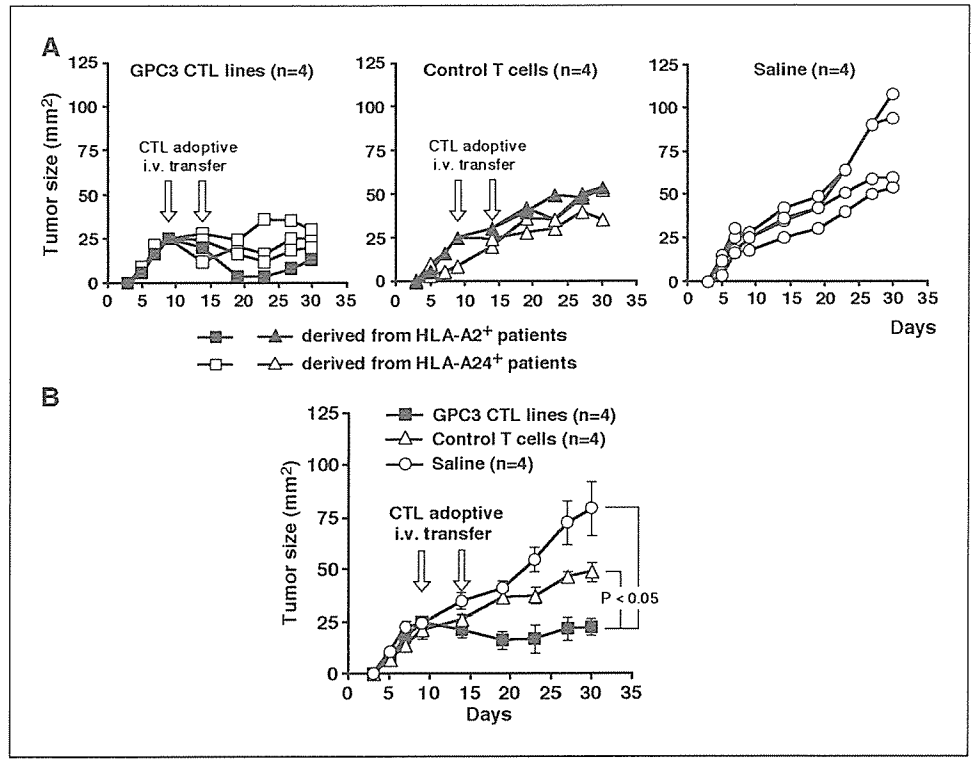

Fig. 4. Marked inhibition of growth of a GPC3-transfected human HCC cancer cell line, SK-Hep1/GPC3, engrafted into NOD/SCID mice after adoptive transfer of human CTLs induced by the GPC3 peptides. *A*, when tumor size reached 25 mm^2 on day 9 after s.c. tumor implantation, human CTLs (3×10^6) reactive to HLA-A2-restricted (■) GPC3 peptide and generated from one HLA-$A2^+$ donor, or those reactive to HLA-A24-restricted (□) GPC3 peptide and pooled from two HLA-$A24^+$ donors were i.v. inoculated. On day 14, the inoculation of CTLs generated from the donors distinct from those at the first injection was repeated. The control $CD8^+$ T cells stimulated with irrelevant HLA-A2-restricted (▲) or HLA-A24-restricted (△) HIV peptides were also injected into mice as a control. Tumor volumes in NOD/SCID mice given twice on days 9 and 14 with GPC3 epitope peptide – induced CTL lines ($n = 4$), control $CD8^+$ T cells ($n = 4$), or saline alone ($n = 4$). Tumor size was expressed in square millimeters. *B, points,* mean tumor sizes in each group of mice; *bars,* ±SD ($n = 4$). Statistical significance was evaluated using *t* test.

GPC3-reactive CTLs could be generated from PBMCs stimulated with these peptides in ~50% of HCC patients. Vaccination based on these peptides did not induce autoimmunity in HLA-A2.1 (HHD) Tgm of a B57Bl/6 background. We previously identified the $GPC3_{298\text{-}306}$ peptide to be a CTL epitope in BALB/c mouse, and we expected that this GPC3 peptide might also be present in human CTL in a HLA-A24-restricted manner. As expected, we could generate HLA-A24-restricted and the $GPC3_{298\text{-}306}$ peptide-reactive human CTLs in this study. As a result, BALB/c mice may be useful for identifying HLA-A24-restricted CTL epitopes. HLA-A2.1 (HHD) Tgm was reported to be a versatile animal model for the preclinical evaluation of peptide-based immunotherapy (12, 13). We could also find its usefulness for the identification of HLA-A2-restricted antigenic epitope in this study.

In this study, we wanted to identify the most effective major CTL epitopes derived from GPC3. As a result, we used BM-DCs derived from HLA-A2.1 (HHD) Tgm and pulsed BM-DCs with the mixture of GPC3 peptides for the vaccination of mice. Some of the peptides tested stimulated the weak response of CTLs in an ELISPOT assay, and these peptides might also be useful for future analysis. It was recently reported that peptides having a weak affinity to MHC, which could not be predicted by a BIMAS system, could induce peptide-reactive CTLs with a cytotoxic activity (27). To search for more peptides that can be applicable for immunotherapy, it may be necessary to check these minor CTL epitopes in the future. In this study, the GPC3-derived peptides predicted to have high binding affinity to HLA-A2 molecules and having the amino acid sequences conserved between human and mouse GPCs were selected for the analysis. When we analyzed the amino acid sequence of human GPC3 protein, all of the top 28 human GPC3 peptides having high binding scores (>100) to HLA-A2 molecules shared the same amino acid sequences with mouse GPC3. Therefore, it is unlikely that we excluded many candidates of human GPC3-derived and HLA-A2-restricted CTL epitopes from the analysis by selecting the peptides having amino acid sequences shared between human and mouse GPC3. Furthermore, we have to consider the differences in the T cell repertoire in mice and humans. Thereby, we may miss GPC3 peptides recognized by human CTLs but not by mouse CTLs.

Considering ideal immunogenic target molecules for cancer immunotherapy, it is important to select a tumor antigen that could not be lost by tumor cells through immunoediting (28, 29). Recently, Capurro et al. reported that GPC3 is involved in the carcinogenesis and proliferation of HCC via regulation of noncanonical Wnt signals (30). Therefore, it may be possible that tumor cells cannot lose the GPC3 expression in order to continue to grow. Furthermore, according to an immunohistochemical analysis of the expression of HLA-class I molecules using newly developed specific mAb, EMR 8-5,[5] we found that almost all HCC cells expressed HLA-class I as far as we could examine (Table 2). For these reasons, we think that GPC3 is a very useful candidate as a target tumor antigen for the immunotherapy of HCC. We and others previously reported that the expression of GPC3 in HCC was detected from an early stage and the quantification of the soluble GPC3 protein in sera was useful for a diagnosis of HCC at an early stage (5, 7). As a result, GPC3-based immunotherapy might be able to prevent the appearance of HCC in patients with hepatitis B or C–based liver cirrhosis.

In this study, we found that it is possible to induce GPC3-reactive CTLs by the stimulation of PBMCs with the two major GPC3 epitopes *in vitro* in 50% of the HCC patients having an appropriate *HLA-class I* allele. However, it is necessary to investigate more patients to estimate the probability of a

successful induction of GPC3-reactive CTLs in HCC patients. We intended to know whether there was any correlation between successful induction of GPC3 peptide-reactive CTLs and prognosis or CTL infiltration into tumor tissue of these patients, therefore, we investigated the seven index cases; patients A2-10, A24-1, A24-2, A24-4, A24-9, A24-11, and A24-12, to see whether there was any correlation between successful induction of GPC3 peptide-reactive CTLs and prognosis or CTL infiltration into the tumor tissue of these patients. In three patients, A24-1, A24-4, and A24-12, who could generate GPC3 peptide-reactive CTLs, patient A24-12 recurred at 6 months after operation. In four patients, A2-10, A24-2, A24-9, and A24-11, who failed to induce GPC3-peptide-reactive CTLs, patient A24-9, whose HCC did not express GPC3, recurred at 6 months after operation, and patient A24-2 recurred at 3 months after operation and died 3 months after recurrence. These three recurred patients had extremely strong tumor invasion to the vasculature. Therefore, it was difficult to evaluate the correlation between the positive CTL response and clinical improvement at the present stage, and we have to increase the number of patients investigated and to do further statistical analyses on these relationships. In patients who could be examined for the infiltration of CD8-positive cells into their tumor specimens and for the existence of terminal deoxynucleotidyl transferase-mediated nick end labeling-positive cells in tumor tissue, patients A2-10, A24-1, A24-2, and A24-9, there was no strong correlation between the positive GPC3 peptide-reactive CTL response and for the existence of CD8-positive or terminal deoxynucleotidyl transferase-mediated nick end labeling-positive cells in the tumor tissues (data not shown). As shown in Fig. 4, we observed a regression of the tumor masses in NOD/SCID mice implanted with SK-Hep1/GPC3 and transferred i.v. with the GPC3 peptide-reactive CTLs in comparison to the mice injected with control $CD8^+$ T cells or saline alone. Although the regression of tumor growth was observed for 2 weeks after the second transfer of CTLs, the tumors began to enlarge again after that period. We thought it was important to continue the transfer of CTLs again and again to obtain continuous regression of the GPC3-expressing tumor. These data suggest that the adoptive i.v. transfer of GPC3-reactive CTLs into mice bearing $GPC3^+$ tumors was useful to inhibit tumor growth in the mouse tumor model.

In addition, it is most important to confirm the usefulness of GPC3-specific *in vivo* cancer immunotherapy in patients with HCC. Investigation of the presence of GPC3-specific CTLs in patients with melanoma are also eagerly awaited. We previously reported that DC differentiated *in vitro* from mouse embryonic stem cells transfected with the mouse *GPC3* gene (24, 31) induced protective immunity against mouse melanoma cell line B16 F10 (32). We are now preparing a translational study of GPC3-based immunotherapy to reduce the risk of recurrence in HCC patients treated surgically. We will try to use the GPC3 epitope peptides identified in this study first, whereas in the second phase, we will make a trial of the peptide-pulsed DC vaccine. We expect that GPC3-based immunotherapy may be a novel treatment strategy that could potentially help to prevent the appearance, advance, and/or recurrence of HCC and melanoma.

Acknowledgments

We thank Dr. Masafumi Takiguchi (Kumamoto University, Kumamoto, Japan), Kyogo Itoh (Kurume University, Kurume, Japan), and the Cell Resource Center for Biomedical Research Institute of Development, Aging and Cancer, Tohoku University for providing the cell lines; Dr. F.A. Lemonnier. (Dapartment SIDA-Retrovirus, Unite d' Immunite Cellulaire Antivirale, Institut Pasteur, France) for providing HLA-A2.1 (HHD) transgenic mice; Tatsuko Kubo (Department of Molecular Pathology, Kumamoto University) for technical assistance with immunohistochemical analyses, and Dr. Mikio Monji (Department of Immunogenetics, Graduate School of Medical Sciences, Kumamoto University) for helpful comments on technical procedures.

References

1. Schafer DF, Sorrell MF. Hepatocellular carcinoma. Lancet 1999;353:1253-7.
2. Tung-Ping Poon R, Fan ST, Wong J. Risk factors, prevention, and management of postoperative recurrence after resection of hepatocellular carcinoma. Ann Surg 2000;232:10-24.
3. Tsao H, Atkins MB, Sober AJ. Management of cutaneous melanoma. N Engl J Med 2004;351:998-1012.
4. Jemal A, Murray T, Ward E, et al. Cancer statistics. CA Cancer J Clin 2005;55:10-30.
5. Hippo Y, Watanabe K, Watanabe A, et al. Identification of soluble NH_2-terminal fragment of glypican-3 as a serological marker for early-stage hepatocellular carcinoma. Cancer Res 2004;64:2418-23.
6. Capurro M, Wanless IR, Sherman M, et al. Glypican-3: a novel serum and histochemical marker for hepatocellular carcinoma. Gastroenterology 2003;125:89-97.
7. Nakatsura T, Yoshitake Y, Senju S, et al. Glypican-3, overexpressed specifically in human hepatocellular carcinoma, is a novel tumor marker. Biochem Biophys Res Commun 2003;306:16-25.
8. Nakatsura T, Kageshita T, Ito S, et al. Identification of glypican-3 as a novel tumor marker for melanoma. Clin Cancer Res 2004;10:6612-21.
9. Zhu ZW, Friess H, Wang L, et al. Enhanced glypican-3 expression differentiates the majority of hepatocellular carcinomas from benign hepatic disorders. Gut 2001;48:558-64.
10. Nakatsura T, Komori H, Kubo T, et al. Mouse homologue of a novel human oncofetal antigen, glypican-3, evokes T-cell-mediated tumor rejection without autoimmune reactions in mice. Clin Cancer Res 2004;10:8630-40.
11. Browning M, Krausa P. Genetic diversity of HLA-A2: evolutionary and functional significance. Immunol Today 1996;17:165-70.
12. Pascolo S, Bervas N, Ure JM, Smith AG, Lemonnier FA, Perarnau B. HLA-A2.1-restricted education and cytolytic activity of CD8(+) T lymphocytes from β2 microglobulin (β2m) HLA-A2.1 monochain transgenic H-2Db β2m double knockout mice. J Exp Med 1997;185:2043-51.
13. Firat H, Garcia-Pons F, Tourdot S, et al. H-2 class I knockout, HLA-A2.1-transgenic mice: a versatile animal model for preclinical evaluation of antitumor immunotherapeutic strategies. Eur J Immunol 1999;29:3112-21.
14. Henderson RA, Michel H, Sakaguchi K, et al. HLA-A2.1-associated peptides from a mutant cell line: a second pathway of antigen presentation. Science 1992;255:1264-6.
15. Karaki S, Kariyone A, Kato N, Kano K, Iwakura Y, Takiguchi M. HLA-B51 transgenic mice as recipients for production of polymorphic HLA-A, B-specific antibodies. Immunogenetics 1993;37:139-42.
16. Wadee AA, Paterson A, Coplan KA, Reddy SG. HLA expression in hepatocellular carcinoma cell lines. Clin Exp Immunol 1994;97:328-33.
17. Matsui M, Machida S, Itani-Yohda T, Akatsuka T. Downregulation of the proteasome subunits, transporter, and antigen presentation in hepatocellular carcinoma, and their restoration by interferon-γ. J Gastroenterol Hepatol 2002;17:897-907.
18. Bourgault Villada I, Moyal Barracco M, Ziol M, et al. Spontaneous regression of grade 3 vulvar intraepithelial neoplasia associated with human papillomavirus-16-specific CD4(+) and CD8(+) T-cell responses. Cancer Res 2004;64:8761-6.
19. Yoshitake Y, Nakatsura T, Monji M, et al. Proliferation potential-related protein, an ideal esophageal cancer antigen for immunotherapy, identified using complementary DNA microarray analysis. Clin Cancer Res 2004;10:6437-48.
20. Monji M, Nakatsura T, Senju S, et al. Identification of a novel human cancer/testis antigen, KM-HN-1, recognized by cellular and humoral immune responses. Clin Cancer Res 2004;10:6047-57.
21. Makita M, Hiraki A, Azuma T, et al. Antilung cancer effect of WT1-specific cytotoxic T lymphocytes. Clin Cancer Res 2002;8:2626-31.
22. Gomi S, Nakao M, Niiya F, et al. A cyclophilin B gene encodes antigenic epitopes recognized by HLA-A24-restricted and tumor-specific CTLs. J Immunol 1999;163:4994-5004.
23. Kai M, Nakatsura T, Egami H, Senju S, Nishimura Y, Ogawa M. Heat shock protein 105 is overexpressed in a variety of human tumors. Oncol Rep 2003;10:1777-82.
24. Matsuyoshi H, Senju S, Hirata S, Yoshitake Y, Uemura Y, Nishimura Y. Enhanced priming of antigen-specific CTLs *in vivo* by embryonic stem cell-derived dendritic cells expressing chemokine along with antigenic

protein: application to antitumor vaccination. J Immunol 2004;172:776–86.
25. Guermonprez P, Valladeau J, Zitvogel L, Thery C, Amigorena S. Antigen presentation and T cell stimulation by dendritic cells. Annu Rev Immunol 2002; 20:621–67.
26. Thomas AM, Santarsiero LM, Lutz ER, et al. Mesothelin-specific CD8(+) T cell responses provide evidence of *in vivo* cross-priming by antigen-presenting cells in vaccinated pancreatic cancer patients. J Exp Med 2004;200:297–306.
27. Bredenbeck A, Losch FO, Sharav T, et al. Identification of noncanonical melanoma-associated T cell epitopes for cancer immunotherapy. J Immunol 2005; 174:6716–24.
28. Kawakami Y, Rosenberg SA. Human tumor antigens recognized by T-cells. Immunol Res 1997;16:313–39.
29. Tsuboi A, Oka Y, Udaka K, et al. Enhanced induction of human WT1-specific cytotoxic T lymphocytes with a 9-mer WT1 peptide modified at HLA-A*2402-binding residues. Cancer Immunol Immunother 2002; 51:614–20.
30. Capurro MI, Xiang YY, Lobe C, Filmus J. Glypican-3 promotes the growth of hepatocellular carcinoma by stimulating canonical Wnt signaling. Cancer Res 2005;65:6245–54.
31. Senju S, Hirata S, Matsuyoshi H, et al. Generation and genetic modification of dendritic cells derived from mouse embryonic stem cells. Blood 2003; 101:3501–8.
32. Motomura Y, Senju S, Nakatsura T, et al. Embryonic stem cell-derived dendritic cells expressing Glypican-3, a recently identified oncofetal antigen, induce protective immunity against highly metastatic mouse melanoma, B16–10. Cancer Res 2006;66: 2414–22.

Embryonic Stem Cell–Derived Dendritic Cells Expressing Glypican-3, a Recently Identified Oncofetal Antigen, Induce Protective Immunity against Highly Metastatic Mouse Melanoma, B16-F10

Yutaka Motomura,[1] Satoru Senju,[1] Tetsuya Nakatsura,[1] Hidetake Matsuyoshi,[1] Shinya Hirata,[1] Mikio Monji,[1] Hiroyuki Komori,[1] Daiki Fukuma,[1] Hideo Baba,[2] and Yasuharu Nishimura[1]

Departments of [1]Immunogenetics and [2]Gastroenterological Surgery, Graduate School of Medical Sciences, Kumamoto University, Kumamoto, Japan

Abstract

We have recently established a method to generate dendritic cells from mouse embryonic stem cells. By introducing exogenous genes into embryonic stem cells and subsequently inducing differentiation to dendritic cells (ES-DC), we can now readily generate transfectant ES-DC expressing the transgenes. A previous study revealed that the transfer of genetically modified ES-DC expressing a model antigen, ovalbumin, protected the recipient mice from a challenge with an ovalbumin-expressing tumor. In the present study, we examined the capacity of ES-DC expressing mouse homologue of human glypican-3, a recently identified oncofetal antigen expressed in human melanoma and hepatocellular carcinoma, to elicit protective immunity against glypican-3-expressing mouse tumors. CTLs specific to multiple glypican-3 epitopes were primed by the *in vivo* transfer of glypican-3-transfectant ES-DC (ES-DC-GPC3). The transfer of ES-DC-GPC3 protected the recipient mice from subsequent challenge with B16-F10 melanoma, naturally expressing glypican-3, and with glypican-3-transfectant MCA205 sarcoma. The treatment with ES-DC-GPC3 was also highly effective against i.v. injected B16-F10. No harmful side effects, such as autoimmunity, were observed for these treatments. The depletion experiments and immunohistochemical analyses suggest that both $CD8^+$ and $CD4^+$ T cells contributed to the observed antitumor effect. In conclusion, the usefulness of glypican-3 as a target antigen for antimelanoma immunotherapy was thus shown in the mouse model using the ES-DC system. Human dendritic cells expressing glypican-3 would be a promising means for therapy of melanoma and hepatocellular carcinoma. (Cancer Res 2006; 66(4): 2414-22)

Introduction

To establish effective immunotherapy for cancer, it is absolutely imperative to identify ideal tumor-specific antigens as targets of antitumor immunotherapy. In addition, the development of the methods to direct immune responses toward the antigens is essential. The manipulation of dendritic cells, specialized antigen-presenting cells, is one of the promising strategies to improve the efficacy of immunotherapy for cancer (1). Currently, numerous reports have shown that dendritic cells loaded with dead tumor cells, tumor cell lysates, tumor antigenic proteins, or peptides can induce immunity and clinical responses (2–5). However, these vaccines often induce a weak immune response that is insufficient for clinical therapy because many tumor antigens are self-antigens against which the immune system has acquired tolerance (6, 7). For loading tumor antigens to dendritic cells for anticancer immunotherapy, the gene-based antigen expression by dendritic cells is considered to be superior to loading antigen as a peptide, protein, or tumor cell lysate (8). For the efficient gene transfer to dendritic cells, the use of virus-based vectors is required because dendritic cells is relatively unsuitable for genetic modification. Clinical trials using dendritic cells genetically modified with virus vectors (e.g., monocyte-derived dendritic cells introduced with adenovirus vectors encoding for tumor antigens) are now under way (9–11). Considering the broader medical applications of this method, the drawbacks of genetic modification with virus vectors include the potential risk accompanying the use of virus vectors and legal restrictions related to it. As a result, the development of safer and more efficient means is considered to be desirable.

We recently established a novel method for the genetic modification of dendritic cells (12). In this method, we generated dendritic cells from mouse embryonic stem cells by *in vitro* differentiation. The levels of expression of MHC molecules and costimulatory molecules, CD80 and CD86, in embryonic stem cell–derived dendritic cells (ES-DC) were comparable with those of bone marrow–derived dendritic cells (BM-DC; ref. 12). The capacity of ES-DC to simulate T cells was comparable with that of dendritic cells generated *in vitro* from BM-DC. We can readily generate genetically modified ES-DC by introducing expression vectors into embryonic stem cells and the subsequent induction of their differentiation into ES-DC (13, 14). The transfection of embryonic stem cells can be done with electroporation using plasmid vectors, and the use of virus-based vectors is not necessary. Once a proper embryonic stem cell transfectant clone is established, it then serves as an infinite source for genetically modified dendritic cells. In a previous study, we showed that the *in vivo* transfer of ES-DC expressing a model tumor antigen, ovalbumin, potently primed ovalbumin-specific CTLs, thereby eliciting a protective effect against ovalbumin-expressing tumor cells (13).

Many of the genes or gene families encoding many cancer/testis antigen or oncofetal antigens have thus far been identified and regarded as ideal targets for anticancer immunotherapy (15–18). However, only a few tumor-associated antigens have been reported as the inducer of both $CD8^+$ and $CD4^+$ T-cell-mediated immune responses (19–22). Recently, we and other groups found that an oncofetal protein glypican-3, glycosylphosphatidylinositol (GPI)–anchored membrane protein, is specifically overexpressed in human

Requests for reprints: Satoru Senju and Yasuharu Nishimura, Department of Immunogenetics, Graduate School of Medical Sciences, Kumamoto University, Kumamoto 860-8556, Japan. Phone: 81-96-373-5313; Fax: 81-96-373-5314; E-mail: senjusat@gpo.kumamoto-u.ac.jp and mxnishim@gpo.kumamoto-u.ac.jp.

doi:10.1158/0008-5472.CAN-05-2090

hepatocellular carcinoma (23, 24). In a subsequent study, we revealed that glypican-3 is overexpressed also in human melanoma (25). An immunohistochemical analysis revealed that the tissue distribution of murine glypican-3 protein was very similar to that in humans. In a previous study, we showed that the *in vivo* transfer of glypican-3 peptide-pulsed BM-DC or glypican-3-reactive CTL line had a potent effect to protect the recipient mice from the murine glypican-3-transfected Colon 26, a colorectal cancer cell line (17).

In the current study, we found that a mouse melanoma cell line F10, which is a subline of B16, naturally expressed glypican-3. Using this cell line as a target, we elucidated the antitumor effect of therapy with ES-DC genetically modified to express murine glypican-3.

Materials and Methods

Mice. CBA and C57BL/6 mice were obtained from Clea Animal Co. (Tokyo, Japan) or Charles River (Hamamatsu, Japan) and maintained under specific pathogen-free conditions. Male CBA and female C57BL/6 mice were mated to produce (CBA × C57BL/6) F1 (CBF1) mice and all studies were done with the F1 mice syngeneic to the mouse embryonic stem cell line TT2 at 6 to 8 weeks of age. The mouse experiments met with approval by Animal Research Committee of Kumamoto University.

Cell lines. The embryonic stem cell line TT2, derived from CBF1 blastocysts (26), was maintained as described previously (12). The method for induction of differentiation *in vitro* of embryonic stem cells into dendritic cells was done as described previously (12), and ES-DC prepared from a 14-day culture in bacteriologic Petri dishes in the presence of granulocyte-macrophage colony-stimulating factor (GM-CSF) were used for *in vivo* and *in vitro* assays. C57BL/6-derived tumor cell lines, F1 and F10 sublines of B16 melanoma, a fibrosarcoma cell line MCA205 (MCA), Lewis lung cancer (3LL) and a thymoma cell line EL4, and a human hepatocellular carcinoma cell line HepG2 were provided by the Cell Resource Center for Biomedical Research Institute of Development, Aging, and Cancer, Tohoku University (Sendai, Japan). The cells were cultured in RPMI 1640 supplemented with 10% FCS. To produce glypican-3-expressing MCA (MCA-GPC3), MCA cells were transfected with pCAGGS-GPC3-internal ribosomal entry site (IRES)-puromycin-resistant (puro-R) by using LipofectAMINE 2000 reagent (Invitrogen Corp., Carlsbad, CA), selected with puromycin, and then subjected to cloning by limiting dilution in drug-free medium using 96-well culture plates (27, 28).

Generation of ES-DC expressing glypican-3. A full-length murine *glypican-3* cDNA clone was purchased from Invitrogen. A cDNA fragment encoding total glypican-3 protein was isolated from that and transferred to a mammalian expression vector pCAGGS-IRES-puro-R, containing the CAG promoter and an IRES-puro-R *N*-acetyltransferase gene cassette (29, 30), to generate an expression vector for *glypican-3*, pCAGGS-GPC3-IRES-puro-R. To generate *glypican-3*-transfected embryonic stem cell clones, TT2 embryonic stem cells were introduced with pCAGGS-GPC3-IRES-puro-R by electroporation and selected with puromycin as described previously (12). *Glypican-3*-transfectant embryonic stem cell clones were subjected to a differentiation culture to generate ES-DC as described previously (12–14). No maturation stimuli, such as lipopolysaccharide or tumor necrosis factor-α, were given to ES-DC before *in vivo* transfer. The expression of *glypican-3* in transfectant ES-DC was confirmed by reverse transcription-PCR (RT-PCR).

RT-PCR and Northern blotting. Total cellular RNA was extracted and RT-PCR was done as described previously (13, 14). Briefly, total RNA was converted into cDNA and PCR was done for 33 cycles for the quantification of *glypican-3* mRNA and for 30 cycles for the quantification of glyceraldehyde-3-phosphate dehydrogenase (*GAPDH*) mRNA. The primer sequences were as follows: *glypican-3*, sense 5′-CTGACTGACCGCGTTACTCCCACA-3′ and antisense 5′-TAGCAGCATCGCCACCAGCAAGCA-3′ and *GAPDH*, sense 5′-GGAAAGCTGTGGCGTGATG-3′ and antisense 5′-CTGTTGCTGTAGCCGTATTC-3′. The sense strand primer used for detection of transgene-derived mRNA was corresponding to the 5′ untranslated region included in the vector DNA. PCR products were visualized by ethidium bromide staining after separation over a 1% agarose gel. A Northern blot analysis was done as described previously (31). In brief, RNA samples (20 μg total RNA per lane) were subjected to electrophoresis in formalin-MOPS gels, blotted onto nylon membranes (Hybond N$^+$, Amersham, Piscataway, NJ), and probed with ^{32}P-labeled DNA probe. A human *glypican-3* cDNA fragment (bp 1,639-2,139) was used as a probe. Human and murine *glypican-3* have a 90% similarity in nucleotide sequence and human cDNA probe hybridized to both human and murine *glypican-3* mRNA.

Peptides, protein, and cytokines. Eleven kinds of 9- to 10-mer glypican-3-derived peptides predicted to bind with H2-D^b or K^b were selected based on the binding score as calculated by the BIMAS software package (BioInformatics and Molecular Analysis Section, Center for Information Technology, NIH, Bethesda, MD). The peptides were synthesized by the F-MOC method on an automatic peptide synthesizer (PSSM8; Shimadzu, Kyoto, Japan) and subsequently purified by high-performance liquid chromatography. The synthetic peptides were designated as murine glypican-3-1 to -11 in ascending order of high binding score. Their amino acid sequences are as follows: murine glypican-3-1, AMFKNNYPSL; murine glypican-3-2, LGSDINVDDM; murine glypican-3-3, LTARINMEQL; murine glypican-3-4, SVLDINECL; murine glypican-3-5, TLCWNGQEL; murine glypican-3-6, YVQKNGGKL; murine glypican-3-7, GMVKVKNQL; murine glypican-3-8, RNGMKNQFNL; murine glypican-3-9, AMLLGLGCL; murine glypican-3-10, ASMELKFLI; and murine glypican-3-11, LFPVIYTQM. Murine glypican-3-11 is predicted to be restricted to H2-K^b and the others to H2-D^b. Recombinant human glypican-3 protein was purchased from R&D Systems (Minneapolis, MN). Recombinant murine GM-CSF and IFN-γ were purchased from PeproTech (London, United Kingdom).

Immunohistochemical and flow cytometric analysis. An immunofluorescence analysis to detect the expression of glypican-3 was done as described previously (16). Anti-human glypican-3 polyclonal antibody was purchased from Santa Cruz Biotechnology (Santa Cruz, CA). FITC-labeled goat anti-rabbit IgG (clone ALI4408; Biosource, Camarillo, CA) was used as a second antibody and propidium iodide for nuclear DNA staining. Stained samples were subjected to microscopic analysis on a confocal microscope (Fluoview FV300, Olympus, Tokyo, Japan). Immunohistochemical analysis of frozen tissue sections was done as described previously (13, 23) using monoclonal antibody (mAb) specific to CD4 (L3T4; BD PharMingen, San Diego, CA) or CD8 (Ly-2; BD PharMingen). In the flow cytometric analysis, cell samples were stained and analyzed on a flow cytometer (FACScan; BD Biosciences, Japan) as described previously (12, 14). Antibodies used for staining were as follows: FITC-conjugated mouse anti-mouse H2-D^b (clone CTDb; mouse IgG2a; Caltag, Burlingame, CA), anti-H2-K^b (clone CTKb; mouse IgG2a; Caltag) and anti-I-A^b (clone 3JP; mouse IgG2a; Caltag), R-phycoerythrin (R-PE)–conjugated anti-mouse CD11c (clone N148; hamster IgG; Chemicon, Temecula, CA), R-PE-conjugated anti-mouse CD86 (clone RMMP-2; rat IgG2a; Caltag), FITC-conjugated goat anti-mouse Ig (BD PharMingen), mouse IgG2a control (clone G155-178; BD PharMingen), FITC-conjugated mouse IgG2a control (clone G155-178; BD PharMingen), and R-PE-conjugated hamster IgG control (Immunotech, Marseille, France).

Generation of BM-DC. Generation of dendritic cells from bone marrow cells was done as described previously (17). For loading of synthetic peptides, BM-DC were incubated with a mixture of three kinds of glypican-3 peptides, murine glypican-3-2, -8, and -11 (10 μmol/L each), at 37°C for 2 hours. For loading of recombinant glypican-3 protein, BM-DC were cultured in the presence of glypican-3 protein (2 μg/mL) at 37°C for 12 hours. No maturation stimuli were given to BM-DC before *in vivo* transfer.

Induction of glypican-3-specific CTLs and cytotoxicity assay. The mice were i.p. immunized with 1 × 10^5 ES-DC twice with a 7-day interval. Seven days after the second immunization, spleen cells were isolated from the mice and cultured (2.5 × 10^6 per well) with ES-DC (1 × 10^5 per well) in 24-well culture plates in RPMI supplemented with 10% horse serum, recombinant human interleukin (IL)-2 (100 units/mL), and 2-mercaptoethanol (50 μmol/L). After the culture for 5 days, the cells were recovered and their cytotoxic activity was analyzed by ^{51}Cr release assays using MCA, MCA-GPC3, B16-F1, and B16-F10 as target cells basically by the same method as described previously (12). B16 cells were pretreated with recombinant murine IFN-γ (1,000 units/mL) before use as target cells as

reported previously (32). In some experiments, $CD8^+$ T cells and natural killer (NK) cells were isolated from effector cell preparations by using a magnetic cell sorting system (Miltenyi, Bergisch Gladbach, Germany). Positively selected cells were 95% pure as determined by flow cytometry.

ELISPOT analysis. Glypican-3-specific T cells were induced by a culture of splenocytes isolated from mice immunized with ES-DC-GPC3 by the same way as described above, except that glypican-3-derived peptides (10 μmol/L) were added to the culture instead of ES-DC-GPC3. After 5 days, the frequency of cells producing IFN-γ on stimulation with target cells (EL4 or EL4 pulsed with each peptide, MCA or MCA-GPC3) was assessed by an ELISPOT assay as described previously (33). The spots were automatically counted and subsequently analyzed using the Eliphoto system (Minerva Tech, Tokyo, Japan).

Tumor prevention and treatment. ES-DC-GPC3 or BM-DC (1×10^5) loaded with glypican-3 peptide or protein were transferred i.p. into mice twice on days −14 and −7, and B16-F10 or MCA-GPC3 cells were challenged s.c. into the shaved back region on day 0. The tumor sizes were determined biweekly in a blinded fashion and survival rate or disease free rate was monitored. Tumor index was calculated as follows: tumor index (mm^2) = (length × width). For the i.v. challenge experiments, tumor cells (B16-F10) were injected i.v. on day 0, and 1×10^5 ES-DC-GPC3 were injected i.p. twice on days 3 and 10 as described previously (34).

***In vivo* depletion of $CD4^+$ and $CD8^+$ T cells.** The mice were transferred i.p. twice with 1×10^5 ES-DC-GPC3 on days −14 and −7 and challenged s.c. with 5×10^3 B16-F10 cells on day 0. For the depletion of T-cell subsets *in vivo*, mice were given a total of six i.p. transfers of the ascites (0.1 mL/mouse/transfer) from hybridoma-bearing nude mice or anti-asialo GM1 on days −18, −15, −11, −8, −4, and −1. Antibodies used were rat anti-mouse CD4 mAb (clone GK1.5), rat anti-mouse CD8 mAb (clone 2.43), and rabbit anti-asialo GM1 polyclonal antibody (Wako Japan; 20 μL/mouse/transfer). Normal rat IgG (Sigma-Aldrich, St. Louis, MO; 200 μg/mouse/transfer) was used as a control. The depletion of T-cell subsets by treatment with antibodies was confirmed by a flow cytometric analysis of spleen cells, which showed a >90% specific depletion.

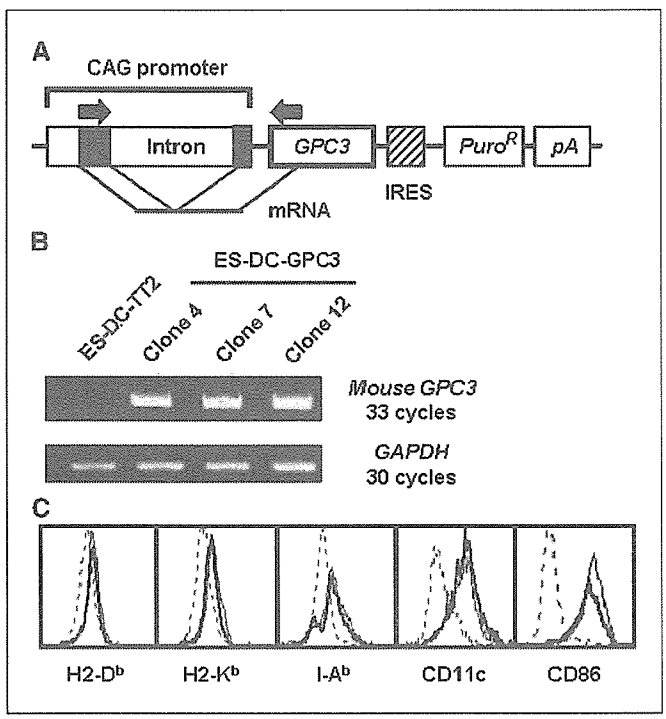

Figure 1. Establishment of ES-DC genetically modified to express murine glypican-3. *A*, structure of pCAGGS-GPC3-IRES-puro-R vector. To obtain pCAGGS-GPC3-IRES-puro-R, a cDNA fragment, including a full-length cDNA of murine *glypican-3*, was inserted into a mammalian expression vector pCAGGS-IRES-puro-R containing the CAG promoter and an IRES-puromycin *N*-acetyltransferase gene cassette. *B*, expression of *glypican-3* mRNA detected by RT-PCR analysis in transfectant ES-DC (ES-DC-GPC3). Primer sets (*arrows* in *A*) were designed to span the intron (917 bp) in the CAG promoter sequence to distinguish PCR products of mRNA origin (249 bp) from the genome-integrated vector DNA origin (1,166 bp). *Black boxes* in (*A*) indicate the 5′-untranslated region of the rabbit β-actin gene included in the CAG promoter. PCR was done at the cycles indicated for quantification of *glypican-3* mRNA and *GAPDH* mRNA. *C*, surface phenotype of genetically modified ES-DC. The expression of the cell surface H2-D^b, H2-K^b, I-A^b, CD11c, and CD86 on transfectant ES-DC was analyzed by a flow cytometric analysis. The staining patterns of ES-DC-GPC3 (*thick line*) closely coincided with those of parental ES-DC (*thin line*). *Dotted lines*, findings for isotype-matched control staining.

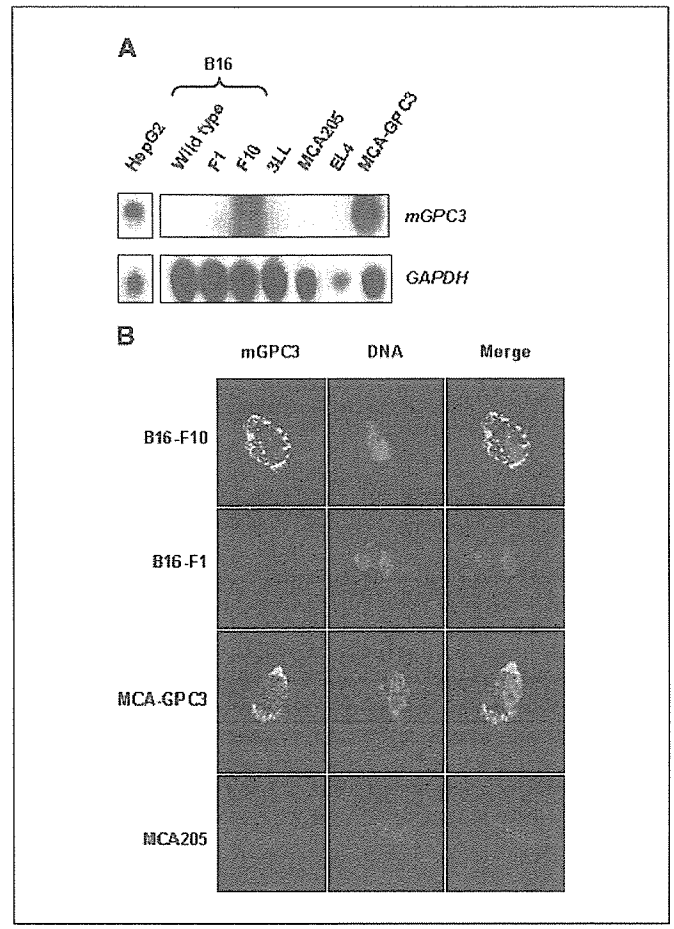

Figure 2. Expression of glypican-3 in cancer cell lines. *A*, Northern blot analysis of *glypican-3* mRNA in a human hepatocellular carcinoma cell line HepG2 (positive control) and various cancer cell lines of C57BL/6 origin. The same filters were stripped and rehybridized with *GAPDH* cDNA to assess the loading of equal amounts of RNA. *B*, immunofluorescence staining analysis of murine glypican-3 protein expressed in B16 variants F1, F10, MCA205, and MCA-GPC3. These cells were stained with rabbit anti-human glypican-3 polyclonal antibody cross-reactive to murine glypican-3 (*green*). Chromosome DNA was visualized by propidium iodide staining (*red*).

Statistical analysis. The two-tailed Student's *t* test was used to determine the statistical significance of differences in the cytolytic activity and tumor growth between the treatment groups. $P < 0.05$ was considered to be significant. The Kaplan-Meier plot for survival was assessed for significance in the tumor challenge experiments using the Breslow-Gehan-Wilcoxon test. Statistical analyses were made using the StatView 5.0 software package (Abacus Concepts, Calabasas, CA).

Results

Generation of ES-DC expressing glypican-3. TT2 embryonic stem cells were introduced with a murine glypican-3 expression vector, pCAGGS-GPC3-IP, driven by the CAG promoter and

containing the IRES-puro-R marker gene (Fig. 1*A*), and several transfectant clones were isolated. The transfectant embryonic stem cell clones were subjected to differentiation to ES-DC, and a transfectant clone 12 expressing the highest level of glypican-3 was selected based on the RT-PCR analysis (Fig. 1*B*). ES-DC differentiated from parental embryonic stem cell line TT2 without transfection were designated as ES-DC-TT2, and ES-DC differentiated from glypican-3-transfectant embryonic stem cells were designated as ES-DC-GPC3. No significant difference was observed in the morphology and levels of the surface expression of H2-D^b, H2-K^b, I-A^b, CD11c, and CD86 between ES-DC-TT2 and ES-DC-GPC3 (Fig. 1*C*). As a result, the transfection of the *glypican-3* gene has little influence on the differentiation of ES-DC.

Expression of glypican-3 in a F10 subline of B16 melanoma. We recently revealed that the oncofetal protein glypican-3 is specifically overexpressed in human hepatocellular carcinomas and melanomas (23, 25). To establish a mouse model system to evaluate the glypican-3 as a target antigen for anticancer immunotherapy, we searched for a transplantable mouse tumor cell line naturally expressing glypican-3. We examined the expression of glypican-3 in several mouse cell lines and found that B16-F10, a subline of B16 melanoma, expressed glypican-3. In a Northern blot analysis, as shown in Fig. 2*A*, where a human hepatocellular carcinoma cell line HepG2 was used as a positive control, *glypican-3* mRNA was evidently detected in a mouse melanoma cell line B16-F10 but not in B16-W.T., B16-F1, 3LL, MCA205, or EL4. The expression of *glypican-3* mRNA was also detected in a glypican-3-transfected MCA, MCA-GPC3. Figure 2*B* shows an immunofluorescence analysis to detect expression of glypican-3 protein. In accordance with the result of the Northern blot analysis, evident expression of glypican-3 protein was detected in B16-F10 and MCA-GPC3. On the other hand, MCA205 and B16-F1 cells did not express glypican-3 protein. Glypican-3 is a GPI-anchored membrane protein, and the results shown in Fig. 2*B* indicated that glypican-3 protein localized at or around cell membrane is

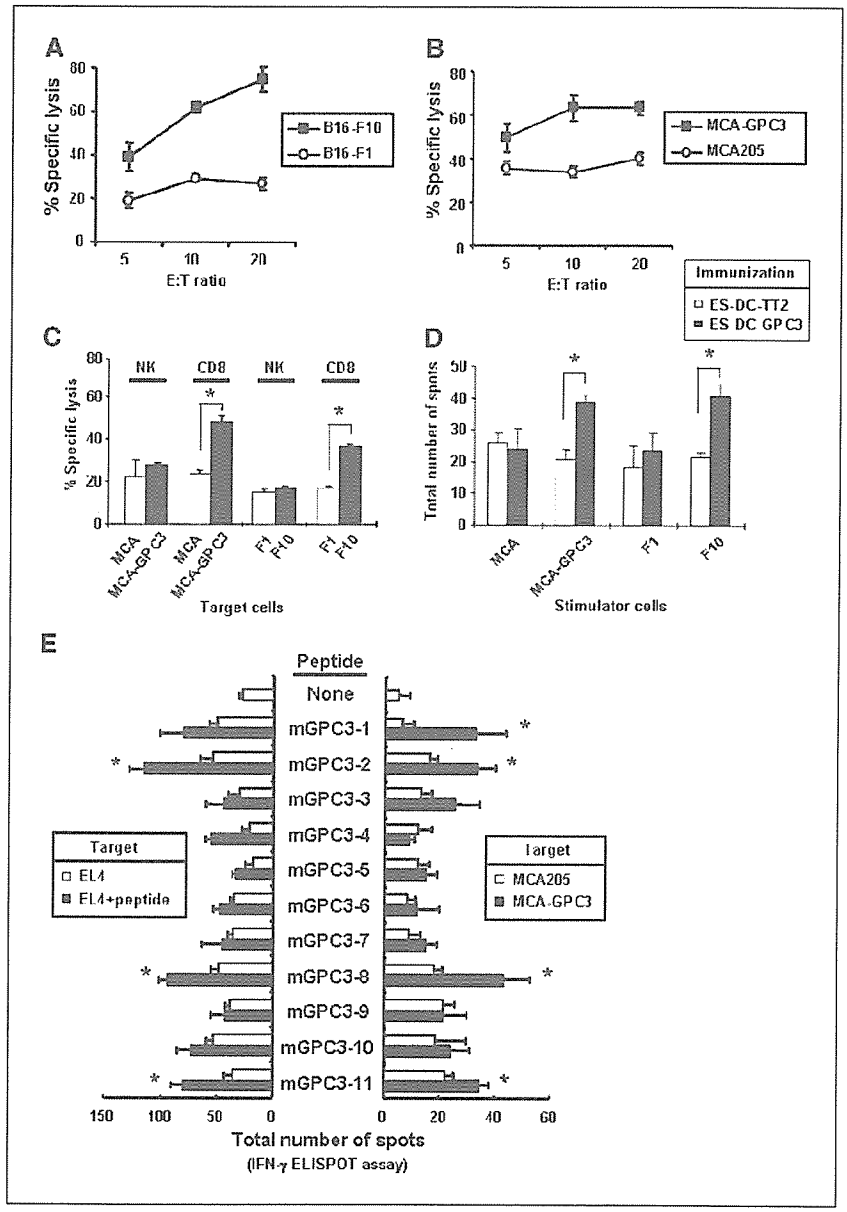

Figure 3. Priming of antigen-specific CTLs with ES-DC-GPC3. The mice were transferred i.p. twice with 1×10^5 ES-DC-GPC3 on days −14 and −7. On day 0, spleen cells from immunized mice were isolated and cultured with 1×10^5 ES-DC-GPC3 per well in the presence of recombinant human IL-2 (100 units/mL) for 5 days. ^{51}Cr release assays were done with the obtained resultant cells to evaluate the capacity to kill IFN-γ pretreated B16-F1 and B16-F10 cells (*A*) and MCA and MCA-GPC3 cells (*B*). Results are expressed as % specific lysis from triplicate assays. *C,* in addition, the resultant cells obtained in the same way were sorted to the fraction of NK cells and $CD8^+$ T cells with microbeads, and another assay was done using the targets in the same condition as in (*A* and *B*). *D,* spleen cells from mice transferred twice with 1×10^5 ES-DC-GPC3 or ES-DC-TT2, respectively, were isolated and restimulated *in vitro* with 1×10^5 ES-DC-GPC3 per well for 5 days. The resultant cells were used for IFN-γ ELISPOT assay. The assay was done in triplicate using the same targets as in (*A* and *B*). *Columns,* mean number of IFN-γ-positive spots. *E,* identification of glypican-3-derived and H2-D^b- or H2-K^b-restricted CTL epitopes by IFN-γ ELISPOT assays. The mice were immunized with 1×10^5 ES-DC-GPC3 twice with a 7-day interval. Spleen cells from mice immunized were restimulated *in vitro* with each glypican-3 peptide (10 μmol/L) and cultured for 5 days with 100 units/mL recombinant human IL-2. ELISPOT assays for 16 hours were examined against EL4 pulsed with or without each peptide and MCA or MCA-GPC3. *Columns,* mean total number of spots from quadruplicate assays. Data are representative of three independent experiments with similar results in (*A-E*). *, $P < 0.05$, differences in the responses are statistically significant between two values in (*C-E*).

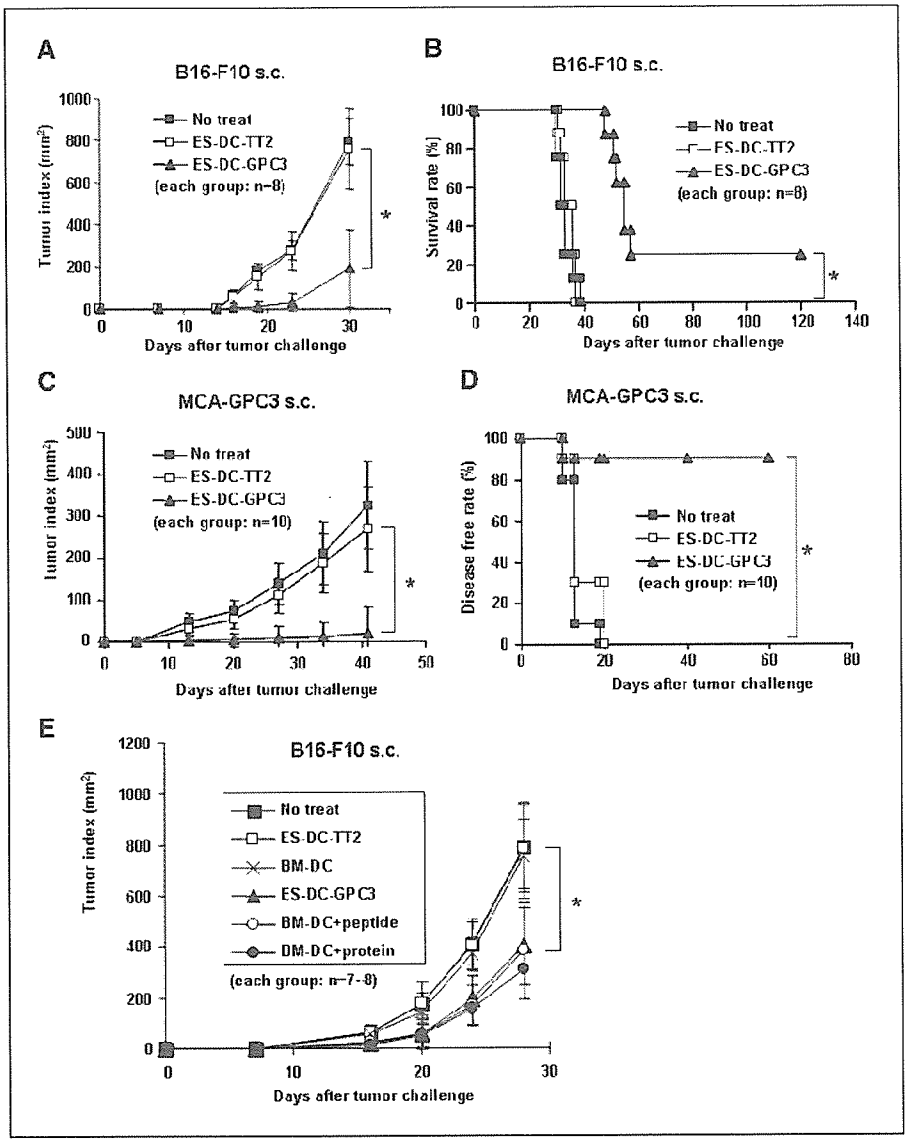

Figure 4. Suppression of tumor growth and prolongation of survival by preimmunization with ES-DC-GPC3. The mice were transferred i.p. twice with 1×10^5 ES-DC-GPC3 or ES-DC-TT2 on days −14 and −7. On day 0, the mice were challenged s.c. with 5×10^3 B16-F10 (*A* and *B*) or 1×10^5 MCA-GPC3 (*C* and *D*) expressing glypican-3. The tumor index, survival rate, or disease-free rate was monitored. *, $P < 0.05$, differences in these three indexes between the groups treated with ES-DC-GPC3 and ES-DC-TT2 were statistically significant. *E*, mice were injected i.p. with ES-DC-GPC3 or BM-DC loaded with a mixture of glypican-3 peptides, murine glypican-3-2, -8, and -11, or glypican-3 protein on the same schedule as in (*A-D*) and challenged s.c. with 5×10^3 B16-F10. Subsequently, the mice were monitored for the growth of tumor.

consistent with this, although some differences in the staining patterns among the cells were observed.

Priming of antigen-specific cytotoxic T cells with genetically modified ES-DC-GPC3. We analyzed the capacity of ES-DC-GPC3 to prime glypican-3-specific CTLs. The mice were immunized i.p. twice with ES-DC-GPC3 or ES-DC-TT2 on days −14 and −7. On day 0, the spleen cells were isolated and restimulated *in vitro* with ES-DC-GPC3 in the presence of exogenous recombinant human IL-2 (100 units/mL). After 5 days, the cells were recovered and their killing activity against target cells with or without expression of glypican-3 was analyzed. As shown in Fig. 3*A* and *B*, the effector cells primed by ES-DC-GPC3 showed a significantly higher killing activity against B16-F10 than against B16-F1, and also against MCA-GPC3 than nontransfectant MCA cells. These results suggest that the effector cells included CTLs recognizing glypican-3. In the experiments shown in Fig. 3*C*, we separated the effector cells into $CD8^+$ T cells and NK cells before the killing assay. NK cells showed activity to kill MCA and MCA-GPC3 in a similar magnitude and to kill B16-F1 and F10 in a similar magnitude, indicating that they killed target cells regardless of glypican-3 expression. On the other hand, for the $CD8^+$ fraction, the cytotoxic activity against B16-F10 was higher than that against B16-F1, and the cytotoxic activity against MCA-GPC3 was higher than that against MCA. On the contrary, spleen cells isolated from mice transferred with ES-DC-TT2 and cocultured *in vitro* with ES-DC-GPC3 exhibited the similar basal levels of killing activities directed against both B16-F1 and F10 as well as MCA and MCA-GPC3 (data not shown).

We next compared the efficiency of the induction of glypican-3-specific and IFN-γ-producing T cells primed by ES-DC-GPC3 with that primed by ES-DC-TT2. The mice were immunized twice with ES-DC-TT2 or ES-DC-GPC3 based on the above described schedule, and the splenocytes isolated from both group of mice were cocultured with ES-DC-GPC3 for 5 days. Thereafter, the frequency of glypican-3-specific T cells was analyzed by an ELISPOT analysis to detect cells producing IFN-γ. As shown in Fig. 3*D*, *in vivo* priming with ES-DC-GPC3 and ES-DC-TT2 resulted in the induction of similar frequency of cells producing IFN-γ on stimulation with cells with no expression of glypican-3, MCA or B16-F1. On the other hand, *in vivo* priming with ES-DC-GPC3 led to the induction of significantly larger number of T cells producing IFN-γ

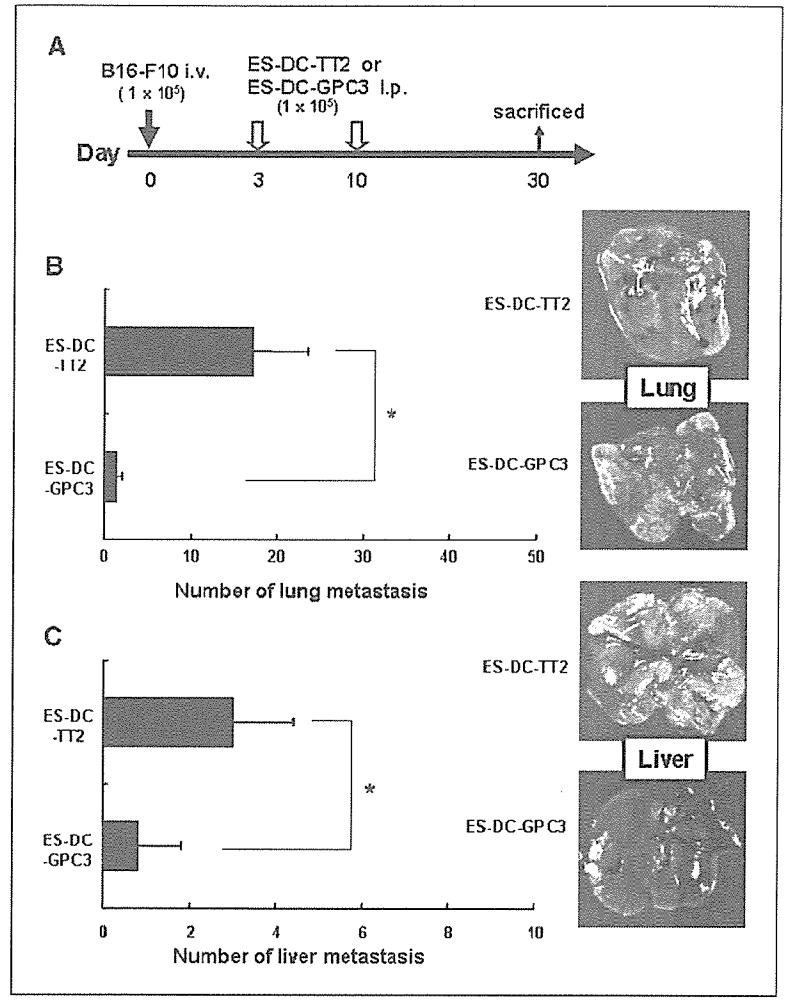

Figure 5. Suppression of tumor growth in the metastatic tumor model of B16-F10. The protocol for therapeutic immunotherapy model was indicated in (*A*). All mice were injected into tail vein with 1×10^5 F10 cells on day 0. On days 3 and 10, mice were injected i.p. with 1×10^5 ES-DC-TT2 or ES-DC-GPC3. On day 30, the mice were sacrificed and the numbers of pulmonary and liver metastases were macroscopically calculated. *Columns,* mean number of total metastases in the lung (*B*) and liver (*C*) using five mice per group. *, $P < 0.05$, differences in the number of metastases are statistically significant between the two values.

on stimulation with cells expressing glypican-3, MCA-GPC3 or B16-F10, compared with priming with ES-DC-TT2. Collectively, these results showed that glypican-3-specific CTLs were primed *in vivo* only when mice were transferred with ES-DC-GPC3, further confirming that ES-DC-GPC3 have the capacity to prime the glypican-3-specific CTLs *in vivo*.

Identification of glypican-3-derived and H2-D^b- or K^b-restricted CTL epitopes. To identify the H-2^b-restricted CTL epitopes of glypican-3, we synthesized 11 glypican-3-derived peptides carrying the binding peptide motifs for H2-D^b or K^b and designated as murine glypican-3-1 to -11 in turn. Spleen cells of the mice immunized with ES-DC-GPC3 by the same procedure as described above were stimulated *in vitro* with each of the peptides instead of ES-DC-GPC3 for 5 days. Subsequently, the frequency of glypican-3-specific CTLs was analyzed by IFN-γ ELISPOT assays. As shown in Fig. 3*E*, cells stimulated *in vitro* with murine glypican-3-2, -8, or -11 showed specific IFN-γ production on restimulation with EL4 cells prepulsed with the same peptide or MCA-GPC3. These results indicate that glypican-3-specific CTLs primed *in vivo* with ES-DC-GPC3 included those recognizing multiple glypican-3 epitopes.

Tumor preventive effects of immunization with ES-DC-GPC3. We next asked whether ES-DC-GPC3 could induce a protective immunity against tumor cells expressing glypican-3 *in vivo*. We immunized mice by the i.p. transfer of ES-DC on days −14 and −7, and the mice were challenged s.c. with 5×10^3 B16-F10 cells or 1×10^5 MCA-GPC3 on day 0. We then monitored the growth of tumors and survival of the mice. As shown in Fig. 4, immunizations with ES-DC-GPC3 provided a significant degree of protection against both B16-F10 and MCA-GPC3. On the other hand, the transfer of ES-DC-TT2 gave no significant protection compared with mice without dendritic cell transfer. Immunization with ES-DC-GPC3 did not show a protective effect against MCA or B16-F1 with no glypican-3 expression (data not shown). Collectively, the *in vivo* administration of ES-DC-GPC3 induced antitumor immunity against glypican-3-expressing tumor cells, thus resulting in a significant inhibition of the growth of tumor and prolongation of the survival time of the treated mice.

Next, we compared ES-DC-GPC3 with BM-DC preloaded with glypican-3 peptide or protein in their capacity to induce antitumor effect. We generated BM-DC from bone marrow cells of CBF1 mice and loaded them with mixture of the three major H2-D^b-restricted epitopes, murine glypican-3-2, -8, and -11 (Fig. 3*E*), or recombinant glypican-3 protein. As shown in Fig. 4*E*, ES-DC-GPC3 and peptide or protein antigen-loaded BM-DC elicited similar magnitude of protective effect against challenge with B16-F10.

Protective effect of ES-DC-GPC3 against i.v. challenge with tumor cells. We next examined the antitumor effect of ES-DC-GPC3 against i.v. challenge with B16-F10. As shown in Fig. 5*A*, the mice were i.v. inoculated with B16-F10 cells on day 0, and the mice were treated with ES-DC-TT2 or ES-DC-GPC3

twice on days 3 and 10. On day 30, mice were sacrificed and macroscopically analyzed. As shown in Fig. 5*B* and *C*, treatment with ES-DC-GPC3 significantly reduced the pulmonary and liver metastases in comparison with the treatment with ES-DC-TT2 ($P < 0.05$). Some of the mice treated with ES-DC-TT2, but not those treated with ES-DC-GPC3, died before they were scheduled to be sacrificed. Thus, the survival time of the mice treated with ES-DC-GPC3 was prolonged in comparison with those treated with ES-DC-TT2.

Identification of effector cells involved in the protection against F10 and MCA-GPC3 induced by ES-DC-GPC3. To determine the subsets of the effector cells involved in the observed protective effect against tumor cells induced by ES-DC-GPC3, we depleted $CD4^+$ or $CD8^+$ T cells in the mice by treatments with either anti-CD4 or anti-CD8 mAb. By this treatment, >90% of $CD4^+$ or $CD8^+$ T cells were depleted (data not shown). The NK cells were depleted by the treatment with anti–asialo GM1 antibody. During this procedure, the mice were immunized with ES-DC-GPC3 and challenged s.c. with B16-F10 cells. As shown in Fig. 6, depletion of $CD4^+$ T cells, $CD8^+$ T cells, or NK cells almost totally abrogated the protective immunity induced by ES-DC-GPC3, suggesting that all of three effector cell subsets were essential for the protective effect.

In a histologic analysis of the tumor tissue specimens, we observed more intense infiltration of inflammatory cells into and/or around tumor tissues of mice immunized with ES-DC-GPC3 than those of mice immunized with ES-DC-TT2. In the metastatic B16-F10 tumor tissue specimens, the infiltrating cells were found to consist of both $CD4^+$ and $CD8^+$ T cells (Fig. 6). These results also suggest that both $CD4^+$ and $CD8^+$ T cells were involved in the antitumor effect against the B16-F10 induced by ES-DC-GPC3.

Discussion

We investigated the antitumor effect of immunization with ES-DC genetically engineered to express a mouse oncofetal antigen glypican-3 against mouse tumor cells naturally expressing GPC3-F10, a subline of B16 melanoma. *In vivo* transfer of ES-DC-GPC3 primed CTL reactive to multiple glypican-3-derived epitopes. The treatment of mice with ES-DC-GPC3 elicited potent protective effect against B16-F10 in both preventive and therapeutic conditions with no evidence of any side effects, such as autoimmunity. The antitumor effect induced by ES-DC-GPC3 was specific to the tumor cells expressing glypican-3, because this treatment was not effective against B16-F1, another subline of B16 with no glypican-3 expression. The glypican-3 specificity of the antitumor effect induced by ES-DC-GPC3 was further confirmed by the observation that the treatment was effective against glypican-3-transfectant MCA205 sarcoma but not against parental MCA 205 cells. The depletion experiments and immunohistochemical analyses showed that $CD8^+$ T cells, $CD4^+$ T cells, and NK cells contributed to the observed antitumor effect.

The tumor cell lines used in this study, MCA205 and B16-F10, were derived from C57BL/6 mice and may be recognized by some fraction of NK cells of CBF1 mice. Thus, the tumor cells must be

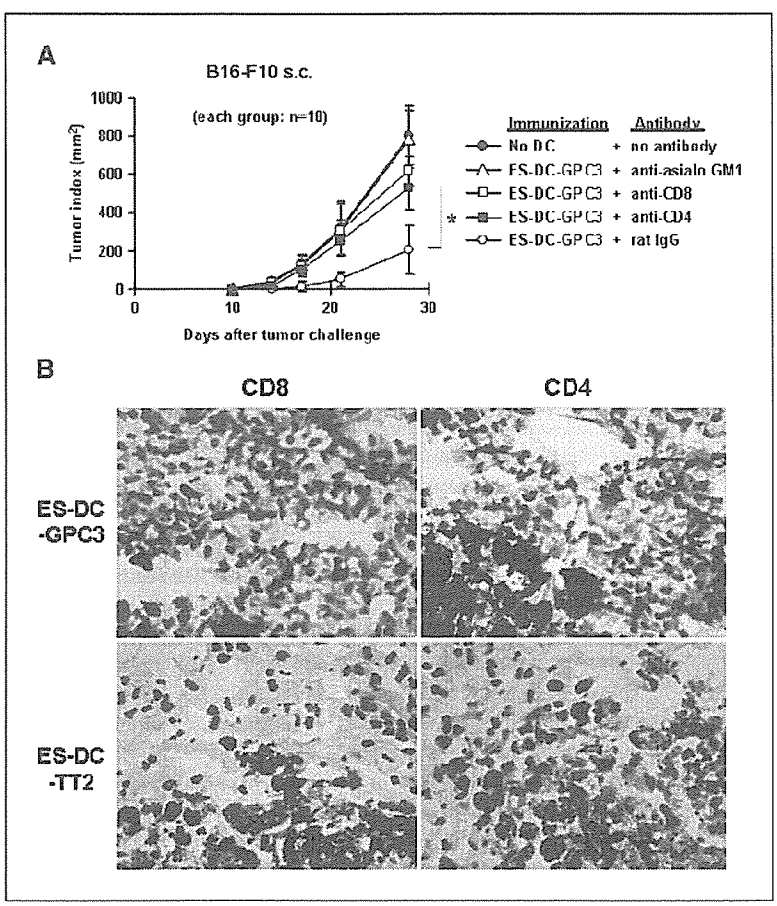

Figure 6. Involvement of both $CD4^+$ and $CD8^+$ T cells in antitumor immunity induced by ES-DC-GPC3. *A*, $CD4^+$ or $CD8^+$ T cells were depleted *in vivo* by the inoculation of anti-CD4 or anti-CD8 mAbs during immunization with ES-DC-GPC3. The mice were challenged s.c. with 5×10^3 F10 tumor cells, and the tumor size was measured and the tumor volume was represented as the tumor index. In immunization with ES-DC-GPC3, the differences in the tumor index between the mice inoculated with rat IgG and those with anti-CD4 mAb or those with anti-CD8 mAb are statistically significant (*, $P < 0.05$). The mice inoculated with anti-CD4 mAb or anti-CD8 mAb showed tumors that were the same size as those in the mice with no transfer with dendritic cells. *Points*, mean tumor index ($n = 10$ per group); *bars*, SD. *B*, infiltration of both $CD4^+$ and $CD8^+$ T cells into pulmonary metastatic tumor tissues. After the challenge with 1×10^5 F10 tumor cells as well as the pulmonary metastatic model in Fig. 5, the mice were treated twice with 1×10^5 ES-DC-TT2 or ES-DC-GPC3. Twenty days after the second treatment, frozen sections of tumor tissue were made and stained with the Giemsa method or immunostained with anti-CD4 or anti-CD8 mAb. In mice treated with ES-DC-GPC3, both $CD8^+$ and $CD4^+$ T cells apparently infiltrated into and/or around the pulmonary metastatic tumor. However, in the mice treated with ES-DC-TT2, neither $CD8^+$ nor $CD4^+$ T cells were detected in the tissue specimens. Magnification, ×400.

more immunogenic to CBF1 mice, used as the recipient mice in the present experiments, than to C57BL/6 mice. However, under the current experimental condition, all of the CBF1 mice challenged with B16-F10 or MCA-GPC3 died unless the recipient mice were treated with ES-DC-GPC3 (Fig. 4*B* and *D*), indicating that these tumor cells are invasive enough also to CBF1 mice.

In the ^{51}Cr release assay shown in Fig. 3*A* to *C*, CTL primed with ES-DC-GPC3 or ES-DC-TT2 (data not shown) exhibited weak killing activity against MCA or B16-F1 cells. Similar weak responses of spleen cells primed with ES-DC-GPC3 or ES-DC-TT2 to MCA or B16-F1 cells were also observed in the ELISPOT assay shown in Fig. 3*D*. At present, we have not yet clarified the effector cells and the target antigens that cause these "background" responses. However, such responses observed *in vitro* did not contribute to the *in vivo* antitumor effect, because the treatment with ES-DC-TT2 had no antitumor effects as shown in Fig. 4.

There was a considerable difference in the effect of treatment with ES-DC-GPC3 between the challenge with B16-F10 and that with MCA-GPC3 cells. This may be partly due to the lower expression of MHC class I on B16 compared with MCA205. B16 does not express MHC class I unless they are stimulated with IFN-γ. The indispensable role of NK cells in the antitumor effect (Fig. 6*A*) suggests that NK cells recognized B16 cells expressing a very low level of MHC class I; subsequently, NK cells produced IFN-γ to up-regulate MHC class I molecules on B16-F10 cells and to make B16-F10 cells sensitive to an attack by glypican-3-specific CTLs (35, 36).

As shown in Fig. 4, the protection against B16-F10 elicited by ES-DC-GPC3 was not complete. Treatment of the ES-DC with some maturation stimuli or loading of α-galactosylceramide, a ligand for NKT cells, to ES-DC before *in vivo* administration may have some effect to enhance the antitumor effect (37). As a future project, we are planning to generate ES-DC genetically engineered to produce cytokines, such as IL-15 or IL-21, along with glypican-3 to improve the antitumor effect.

We reported previously that the induction of immune response to glypican-3 protected the mice from a challenge with Colon 26 colon tumor cells genetically modified to overexpress glypican-3 (17). In the present study, we found the natural overexpression of glypican-3 in B16-F10 and showed that the immunization of mice with glypican-3 protected the mice from the challenge with B16-F10. Glypican-3 is one of the oncofetal proteins and the expression in normal human tissues is limited to the placenta and fetal liver (17). In addition, the tissue distribution of glypican-3 expression is very similar in mice and humans (17). As a result, our results strongly suggest that anti-melanoma and anti–hepatocellular carcinoma immunotherapy with glypican-3 seems to be an effective and safe method, and it should therefore be tested clinically.

To enable to the future clinical application of ES-DC, we recently established a method for generating ES-DC from embryonic stem cells of nonhuman primate, cynomolgus monkey, and also for genetic modification of them.[3] Considering the future clinical application of ES-DC technology, allogenicity (i.e., differences in the genetic background between the patients to be treated and the embryonic stem cells as the source for dendritic cells), we expected to cause problems. However, it is expected that human embryonic stem cells sharing some of HLA alleles with patients are available in most cases. We recently found that antigen-expressing ES-DC could potently prime antigen-specific CTL on the adoptive transfer to semiallogeneic mice, thus sharing some MHC alleles with the ES-DC and also protecting the recipient mice from subsequent challenge with tumor cells bearing the antigen (38). Immunotherapy with human ES-DC expressing glypican-3 may therefore be clinically useful as an immunotherapy of melanoma and hepatocellular carcinoma.

Acknowledgments

Received 6/15/2005; revised 11/27/2005; accepted 12/8/2005.

Grant support: Ministry of Education, Science, Technology, Sports, and Culture, Japan, grants-in-aid 12213111, 14370115, 14570421, and 14657082; Ministry of Health, Labor and Welfare, Japan, Research Grant for Intractable Diseases; Tokyo Biochemical Research Foundation; Uehara Memorial Foundation; Oncotherapy Science Co.; Eisai Pharmasential Co.; and Meiji Institute of Health Science.

The costs of publication of this article were defrayed in part by the payment of page charges. This article must therefore be hereby marked *advertisement* in accordance with 18 U.S.C. Section 1734 solely to indicate this fact.

We thank Dr. S. Aizawa (Riken Center for Developmental Biology, Kobe, Japan) for TT2, Drs. N. Takakura (Kanazawa University, Kanazawa, Japan) and T. Suda (Keio University, Tokyo, Japan) for OP9, Dr. H. Niwa (Riken Center for Developmental Biology) for pCAG-IP, and T. Kubo for technical assistance.

[3] In preparation.

References

1. O'Neill DW, Adams S, Bhardwaj N. Manipulating dendritic cell biology for the active immunotherapy of cancer. Blood 2004;104:2235–46.
2. Wen YJ, Min R, Tricot G, Barlogie B, Yi Q. Tumor lysate-specific cytotoxic T lymphocytes in multiple myeloma: promising effector cells for immunotherapy. Blood 2002;99:3280–5.
3. Asavaroengchai W, Kotera Y, Mulé JJ. Tumor lysate-pulsed dendritic cells can elicit an effective antitumor immune response during early lymphoid recovery. Proc Natl Acad Sci U S A 2002;99:931–6.
4. Zwaveling S, Ferreira Mota SC, Nouta J, et al. Established human papilloma virus type 16-expressing tumors are effectively eradicated following vaccination with long peptides. J Immunol 2002;169:350–8.
5. Prins RM, Odesa SK, Liau LM. Immunotherapeutic targeting of shared melanoma-associated antigens in a murine glioma model. Cancer Res 2003;63:8487–91.
6. Finn OJ. Cancer vaccines: between the idea and the reality. Nat Rev Immunol 2003;3:630–41.
7. Blattman JN, Greenberg PD. Cancer immunotherapy: a treatment for the masses. Science 2004;305:200–5.
8. Murphy A, Westwood JA, Teng MW, Moeller M, Darcy PK, Kershaw MH. Gene modification strategies to induce tumor immunity. Immunity 2005;22:403–14.
9. Bonehill A, Heirman C, Tuyaerts S, et al. Efficient presentation of known HLA class II-restricted MAGE-A3 epitopes by dendritic cells electroporated with messenger RNA encoding an invariant chain with genetic exchange of class II-associated invariant chain peptide. Cancer Res 2003;63:5587–94.
10. Höltl L, Ramoner R, Zelle-Rieser C, et al. Allogeneic dendritic cell vaccination against metastatic renal cell carcinoma with or without cyclophosphamide. Cancer Immunol Immunother 2005;54:663–70.
11. Erhardt M, Gorschlüter M, Sager J, et al. Transfection of human monocyte-derived dendritic cells with CpG oligonucleotides. Immunol Cell Biol 2005;83:278–85.
12. Senju S, Hirata S, Matsuyoshi H, et al. Generation and genetic modification of dendritic cells derived from mouse embryonic stem cells. Blood 2003;101:3501–8.
13. Matsuyoshi H, Senju S, Hirata S, Yoshitake Y, Uemura Y, Nishimura Y. Enhanced priming of antigen-specific CTLs *in vivo* by embryonic stem cell-derived dendritic cells expressing chemokine along with antigenic protein: application to antitumor vaccination. J Immunol 2004;172:776–86.
14. Hirata S, Senju S, Matsuyoshi H, Fukuma D, Uemura Y, Nishimura Y. Prevention of experimental autoimmune encephalomyelitis by transfer of embryonic stem cell-derived dendritic cells expressing myelin oligodendrocyte glycoprotein peptide along with TRAIL or programmed death-1 ligand. J Immunol 2005;174:1888–97.
15. Yamada A, Kawano K, Koga M, Takamori S, Nakagawa M, Itoh K. Gene and peptide analyses of newly defined lung cancer antigens recognized by HLA-A2402-restricted tumor-specific cytotoxic T lymphocytes. Cancer Res 2003;63:2829–35.
16. Monji M, Nakatsura T, Senju S, et al. Identification of a novel human cancer/testis antigen, KM-HN-1, recognized by cellular and humoral immune responses. Clin Cancer Res 2004;10:6047–57.
17. Nakatsura T, Komori H, Kubo T, et al. Mouse homologue of a novel human oncofetal antigen, glypican-3, evokes T-cell-mediated tumor rejection without autoimmune reactions in mice. Clin Cancer Res 2004;10:8630–40.
18. Oberthuer A, Hero B, Spitz R, Berthold F, Fischer M. The tumor-associated antigen PRAME is universally expressed in high-stage neuroblastoma and

associated with poor outcome. Clin Cancer Res 2004; 10:4307–13.
19. Nakatsura T, Senju S, Ito M, Nishimura Y, Itoh K. Cellular and humoral immune responses to a human pancreatic cancer antigen, coactosin-like protein, originally defined by the SEREX method. Eur J Immunol 2002;32:826–36.
20. Maraskovsky E, Sjölander S, Drane DP, et al. NY-ESO-1 protein formulated in ISCOMATRIX adjuvant is a potent anticancer vaccine inducing both humoral and $CD8^+$ T-cell-mediated immunity and protection against NY-ESO-1^+ tumors. Clin Cancer Res 2004;10: 2879–90.
21. Li B, He X, Pang X, Zhang H, Chen J, Chen W. Elicitation of both CD4 and CD8 T-cell-mediated specific immune responses to HCA587 protein by autologous dendritic cells. Scand J Immunol 2004;60:506–13.
22. Daniel D, Chiu C, Giraudo E, et al. $CD4^+$ T cell-mediated antigen-specific immunotherapy in a mouse model of cervical cancer. Cancer Res 2005; 65:2018–25.
23. Nakatsura T, Yoshitake Y, Senju S, et al. Glypican-3, overexpressed specifically in human hepatocellular carcinoma, is a novel tumor marker. Biochem Biophys Res Commun 2003;306:16–25.
24. Capurro M, Wanless IR, Sherman M, et al. Glypican-3: a novel serum and histochemical marker for hepatocellular carcinoma. Gastroenterology 2003;125:89–97.
25. Nakatsura T, Kageshita T, Ito S, et al. Identification of glypican-3 as a novel tumor marker for melanoma. Clin Cancer Res 2004;10:6612–21.
26. Yagi T, Tokunaga T, Furuta Y, et al. A novel ES cell line, TT2, with high germline-differentiating potency. Anal Biochem 1993;214:70–6.
27. Senju S, Iyama K, Kudo H, Aizawa S, Nishimura Y. Immunocytochemical analyses and targeted gene disruption of GTPBP1. Mol Cell Biol 2000;20:6195–200.
28. Bakker J, Lin X, Nelson WG. Methyl-CpG binding domain protein 2 represses transcription from hypermethylated pi-class glutathione *S*-transferase gene promoters in hepatocellular carcinoma cells. J Biol Chem 2002;277:22573–80.
29. Niwa H, Masui S, Chambers I, Smith AG, Miyazaki J. Phenotypic complementation establishes requirements for specific POU domain and generic transactivation function of Oct-3/4 in embryonic stem cells. Mol Cell Biol 2002;22:1526–36.
30. Niwa H, Yamamura K, Miyazaki J. Efficient selection for high-expression transfectants with a novel eukaryotic vector. Gene 1991;108:193–9.
31. Nakatsura T, Senju S, Yamada K, Jotsuka T, Ogawa M, Nishimura Y. Gene cloning of immunogenic antigens overexpressed in pancreatic cancer. Biochem Biophys Res Commun 2001;281:936–44.
32. Böhm W, Thoma S, Leithäuser F, Möller P, Schirmbeck R, Reimann J. T cell-mediated, IFN-γ-facilitated rejection of murine B16 melanomas. J Immunol 1998;161:897–908.
33. Bourgault Villada I, Moyal Barracco M, Villada IB, et al. Spontaneous regression of grade 3 vulvar intraepithelial neoplasia associated with human papillomavirus-16-specific $CD4^+$ and $CD8^+$ T-cell responses. Cancer Res 2004;64:8761–6.
34. Fukui M, Nakano-Hashimoto T, Okano K, et al. Therapeutic effect of dendritic cells loaded with a fusion mRNA encoding tyrosinase-related protein 2 and enhanced green fluorescence protein on B16 melanoma. Tumour Biol 2004;25:252–7.
35. Xu D, Gu P, Pan PY, Li Q, Sato AI, Chen SH. NK and $CD8^+$ T cell-mediated eradication of poorly immunogenic B16-F10 melanoma by the combined action of IL-12 gene therapy and 4-1BB costimulation. Int J Cancer 2004;109:499–506.
36. Corthay A, Skovseth DK, Lundin KU, et al. Primary antitumor immune response mediated by $CD4^+$ T cells. Immunity 2005;22:371–83.
37. Matsuyoshi H, Hirata S, Yoshitake Y, et al. Therapeutic effect of α-galactosylceramide-loaded dendritic cells genetically engineered to express SLC/CCL21 along with tumor antigen against peritoneally disseminated tumor cells. Cancer Sci 2005;96:889–96.
38. Fukuma D, Matsuyoshi H, Hirata S, et al. Cancer prevention with semi-allogeneic ES cell-derived dendritic cells. Biochem Biophys Res Commun 2005;335:5–13.

Synthetic small interfering RNA targeting heat shock protein 105 induces apoptosis of various cancer cells both *in vitro* and *in vivo*

Seiji Hosaka,[1] Tetsuya Nakatsura,[1,4] Hirotake Tsukamoto,[1] Takumi Hatayama,[3] Hideo Baba[2] and Yasuharu Nishimura[1,5]

Departments of [1]Immunogenetics and [2]Gastroenterological Surgery, Graduate School of Medical Sciences, Kumamoto University, 1-1-1 Honjo, Kumamoto 860-8556, and [3]Department of Biochemistry, Kyoto Pharmaceutical University, 5 Nakauchi-cho, Misasagi, Yamashina-ku, Kyoto 607-8414, Japan

(Received December 17, 2005/Revised February 21, 2006/Accepted February 25, 2006/Online publication April 19, 2006)

We previously reported that heat shock protein 105 (HSP105), identified by serological analysis of a recombinant cDNA expression library (SEREX) using serum from a pancreatic cancer patient, was overexpressed in various human tumors and in the testis of adult men by immunohistochemical analysis. In the present study, to elucidate the biological function of the HSP105 protein in cancer cells, we first established NIH3T3 cells overexpressing murine HSP105 (NIH3T3-HSP105). The NIH3T3-HSP105 cells acquired resistance to apoptosis induced by heat shock or doxorubicin. The small interfering RNA (siRNA)-mediated suppression of HSP105 protein expression induced apoptosis in human cancer cells but not in fibroblasts. By a combination of siRNA introduction and doxorubicin or heat shock treatment, apoptosis was induced synergistically in a human colon cancer cell line, HCT116. *In vivo*, siRNA inoculation into the human gastric cancer cell line KATO-3 established in the flank of an NOD SCID mouse suppressed the tumor growth. This siRNA-induced apoptosis was mediated through caspases, but not the p53 tumor suppressor protein, even though the HSP105 protein was bound to wild-type p53 protein in HCT116 cells. These findings suggest that the constitutive overexpression of HSP105 in cancer cells is involved in malignant transformation by protecting tumor cells from apoptosis. HSP105 may thus be a novel target molecule for cancer therapy and a treatment regimen using synthetic siRNA to suppress the expression of HSP105 protein may provide a new strategy for cancer therapy. (*Cancer Sci* 2006; 97: 623–632)

Heat shock protein 105 (also called HSP110)[1] is a stress protein belonging to the HSP105/110 family that is expressed constitutively in most tissues at low levels, whereas HSP105 mRNA is expressed at high levels in mouse and rat brain. At the protein level, high expression levels have been reported only in the brain of mice.[1–4] Like other heat shock proteins, HSP105 plays an important role as a chaperone under physiological conditions. HSP105 is induced by various stressors and plays an important role in protecting cells from the cytotoxic effects mediated by such stressors. HSP105 is composed of an ATP-binding domain, a β-sheet, a loop and α-helical domains similar to those observed in the HSP70 family of proteins, and it binds to non-native protein substrates, thereby preventing the aggregation of denatured protein through an interaction with the β-sheet domain of HSP105.[2,5–7]

The rat neuronal cell line PC12 transfected stably with murine *HSP105* exhibited resistance to caspase-mediated apoptosis induced by stressors.[8] In a spinal and bulbar muscular atrophy model, the transient expression of tAR containing an expanded polyglutamine tract caused aggregates of polyglutamine in COS-7 and SK-N-SH cells and then induced the cells to undergo apoptosis. In contrast, in cells cotransfected with *tAR* and *HSP105*, both the aggregation of polyglutamine and the degree of it's cell toxicity decreased.[9] In contrast, HSP105 has demonstrated apoptosis-enhancing activity during murine embryogenesis.[10–13] These observations suggest that HSP105 is involved in the regulation of apoptosis.

We previously reported that HSP105 is overexpressed in various human tumors, including colon cancer cells but not colorectal adenomas, thus suggesting that the overexpression of HSP105 is a late event in the colorectal adenoma–carcinoma sequence.[14,15] Recent studies have also demonstrated that the expression level of HSP105 is elevated in highly metastatic colon cancer cell lines, and is correlated with advanced clinical stages and positive lymph node involvement.[16]

RNA interference is used widely for manipulating biological systems, and has also been utilized successfully as a therapeutic material in experimental animals.[17–19] Synthetic siRNA strongly inhibits the expression of target proteins when they are transfected with cationic liposomes, which are thought to be safer than viral vectors for human therapy. The local injection of synthetic siRNA against VEGF [20] or sphingosine 1-phosphate receptor-1[21] into established tumors has been reported recently to suppress angiogenesis and tumor growth.

The role of HSP105 in cancer cells has yet to be elucidated. In the present study, we first transfected the *HSP105* gene

[4]T. Nakatsura is currently in the Immunotherapy Section, Investigative Treatment Division Research Center for Innovative Oncology, National Cancer Center Hospital East, Kashiwa City, Chiba, Japan.
[5]To whom correspondence should be addressed.
E-mail: mxnishim@gpo.kumamoto-u.ac.jp

Abbreviations: CML, chronic myelocytic leukemia; DMEM, Dulbecco's modified Eagle's medium; ER, endoplasmic reticulum; FCS, fetal calf serum; FITC, fluorescein-isothiocyanate; GFP, green fluorescent protein; HBSS, Hanks' balanced salt solution; HSP70, heat shock protein 70; HSP105, heat shock protein 105; IRES, internal ribosomal entry site; NIH3T3-HSP105, NIH3T3 cells overexpressing murine HSP105; PARP, poly ADP-ribose polymerase; PBS, phosphate-buffered saline; PI, propidium iodide; RT-PCR, reverse transcription–polymerase chain reaction; SEREX, serological analysis of a recombinant cDNA expression library; siRNA, small interfering RNA; tAR, truncated androgen receptor; VEGF, vascular endothelial growth factor.

doi: 10.1111/j.1349-7006.2006.00217.x

into NIH3T3 cells to examine the function of those cells, while also treating those transfectants with several stressors. To investigate whether the suppression of HSP105 expression affects the growth of cancer cells, we then introduced synthetic siRNA specific to HSP105 into several human cancer cell lines both *in vitro* and *in vivo*. We herein report that HSP105 has an anti-apoptotic function and that an overexpression of HSP105 is essential for cancer cells to survive.

Materials and Methods

Cell lines and culture

The human pancreatic cancer cell line PK8 and the murine fibroblast cell line NIH3T3 were kindly provided by the Cell Resource Center for Biomedical Research Institute of Development, Aging and Cancer, Tohoku University (Sendai, Japan). The human hepatoma cell line SK-Hep1, human colon cancer cell line SW620, and human gastric cancer cell lines KATO-3 and MKN28 were kindly provided by Dr K. Itoh, Kurume University (Kurume, Japan). The human colon cancer cell line HCT116 was kindly provided by Dr B. Vogelstein, Johns Hopkins University (Baltimore, MD, USA). Primary normal fibroblast strains Turu and Mori were kindly provided by Dr M. Yamaizumi, Kumamoto University (Kumamoto, Japan).

NIH3T3, HCT116, SW620, Turu and Mori were all cultured *in vitro* in DMEM, and SK-Hep1, PK8, KATO-3 and MKN28 were cultured in RPMI medium supplemented with 10% FCS and 1% penicillin and streptomycin in a 5% CO_2 atmosphere at 37°C.

Mice

C57BL/6 NOD SCID mice were kindly provided by Dr S. Okada, Kumamoto University. The mice were maintained at the Center for Animal Resources and Development of Kumamoto University and they were handled in accordance with the animal care policy of Kumamoto University.

Plasmid construction and transfection

To obtain pCAGGS-IRES-neo-R, a DNA fragment containing an IRES, the neomycin-resistance gene *neo-R* was inserted into the mammalian expression vector pCAGGS. A cDNA fragment encoding the murine HSP105 protein was inserted into pCAGGS-IRES-neo-R. Cell transfection was carried out using Lipofectamine 2000 (Invitrogen, Carlsbad, CA, USA) according to the manufacturer's recommendations in six-well multiplates. At 48 h after transfection, the cells were replated and were then cultured in the presence of an appropriate concentration of G418 for 1 week.

RT-PCR analysis

Total RNA was isolated using either TRIZOL reagent (Gibco BRL, Rockville, MD, USA) or RNeasy spin column kits (Qiagen, Valencia, CA, USA). Total RNA from normal human colon tissue was purchased from Clontech (Palo Alto, CA, USA). RT-PCR analysis was carried out as described previously.[22] Briefly, 1 μg of total RNA was converted into cDNA in 20 μL of reaction buffer. Each PCR regime involved an initial denaturation step at 94°C for 5 min followed by 24–33 cycles for each type of cDNA. All samples were then processed at 94°C for 1 min, 58°C for 1 min and 72°C for 1 min

The primer sequences were as follows: *HSP105* forward 5′-ATGAAGTGATGGAATGGATG-3′ and reverse 5′-TTTGGTTTCGGTTGTGTTAC; *NOXA* forward 5′-AGATGCCTGGGAAGAAG-3′ and reverse 5′-AGTCCCCTCATGCAAGT-3′; *PUMA* forward 5′-TGTAGAGGAGACAGGAATCCACGG-3′ and reverse, 5′-AGGCACCTAATTGGGCTCCATCTC-3′; *Bax* forward 5′-AGCGGCGGTGATGGACGGGTC-3′ and reverse 5′-TCCAAGGCAGCTGGGGCCTCA-3′; and *p53* forward 5′-CCATGGCCATCTACAAGCAG-3′ and reverse 5′-AGGGTGAAATATTCTCC-3′. PCR products were visualized by ethidium bromide staining after separation on a 2% agarose gel.

Detection of cell apoptosis

Cells in the early phase of apoptosis were detected by staining with annexin V, which binds to a phosphatidyl serine marker specific for the early phase of apoptosis, using an annexin V-FITC apoptosis detection kit (BioVision, Mountain View, CA, USA). The NIH3T3-mock cells and NIH3T3-HSP105 cells were incubated at 45°C for 90 min or with 200 ng/mL doxorubicin. The cancer cell lines were treated with either 100 nM or 200 nM siRNA, with 100 nM siRNA and 200 ng/mL doxorubicin or with 100 nM siRNA and heat shock (45°C, 30 min). The cells were harvested at the times indicated and were then stained with FITC-conjugated annexin V for flow cytometric analysis according to the manufacturer's recommendations. In the caspase inhibition assay, 100 μM Z-VAD-FMK (Sigma, St Louis, MO, USA) was added 1 h before siRNA transfection.

To detect the late phase of apoptosis, DNA fragmentation in the cells was evaluated by staining with PI and flow cytometric analysis as follows: NIH3T3-mock cells and NIH3T3-HSP105 cells treated with doxorubicin were collected by tripsinization, washed with PBS, fixed in cold 70% ethanol, and stored at −20°C until staining. After fixation the cells were washed in PBS and incubated with 100 μg/mL of RNaseA for 30 min at room temperature, before staining with 25 μg/mL of PI. Flow cytometry was carried out using a FACScan flow cytometer (BD Biosciences, San Jose, CA, USA) and the data were analyzed using CellQuest software (BD Biosciences).

Immunoprecipitation and western blot analysis

The cell samples were lysed in appropriate amounts of lysing buffer (200 mM NaCl, 20 mM Tris [pH 7.4], 1% Nonidet P-40, 1 mM sodium orthovanadate [WAKO, Osaka, Japan], 10% glycerol, plus one protease inhibitor tablet [Roche Applied Sciences, Penzberg, Germany]). Hsp105 and p53 were immunoprecipitated with rabbit polyclonal anti-HSP105 antibody and mouse monoclonal anti-p53 antibody (DO-1; Santa Cruz Biotechnology, Santa Cruz, CA, USA), respectively, together with protein A beads (Pierce, Rockford, IL, USA). The proteins were analyzed using 7% or 10% sodium dodecylsulfate–polyacrylamide gel electrophoresis and were then transferred onto a nitrocellulose membrane. HSP105 was blotted with the above-described antibody and PARP was blotted with rabbit polyclonal anti-PARP antibody (Santa Cruz Biotechnology). p53 was blotted with DO-1 or DO-1 and labeled with biotin using the Mini-biotin-XX Protein Labeling Kit (Molecular Probes, Eugene, OR, USA). Phospho-p53 (Ser46) and phospho-p53 (Ser15) were blotted with rabbit polyclonal antibody specific to phospho-p53 (Ser46) and mouse monoclonal antibody specific to phospho-p53 (Ser15) (New England Biolabs, Beverly, MA, USA), respectively, and then with horseradish peroxidase-conjugated rabbit antimouse IgG or donkey antirabbit IgG

doi: 10.1111/j.1349-7006.2006.00217.x

(Amersham Biosciences, Piscataway, NJ, USA), respectively, as secondary antibodies. The bands were visualized by enhanced chemiluminescence (Amersham Biosciences).

siRNA and *in vivo* siRNA treatment

The siRNA duplexes were purchased from Dharmacon Research (HSP105-siRNA and luciferase; Lafayette, CO, USA), Qiagen (GFP) and Invitrogen (HSP105-siRNA-2). The siRNA sequences used were as follows: HSP105, UUGGCUGCAACUCCG-AUUGTT; HSP105-siRNA-2, UGUACAUUACCUUUAUU-CCAACUCC; luciferase, CGUACGCGGAAUACUUCGATT; and GFP, GCAAGCUGACCCUGAAGUUCA. The transfection of siRNA oligonucleotides was carried out using oligofectamine (Invitrogen) according to the manufacturer's recommendations in a six-well plate.

KATO-3 cells (2×10^6) were suspended in 100 μL of HBSS solution (Gibco, Langley, OK, USA), injected subcutaneously into the dorsal skin of NOD SCID mice and were then allowed to grow. After 10 days, siRNA solutions were injected locally into tumors every third day. siRNA solutions were prepared by incubating 1 nmol of siRNA and 20 μL of oligofectamine in 5% glucose solution for 15 min at room temperature. The tumor volume was calculated using the equation

$$V = (L \times W^2) \times 0.5,$$

where V = volume, L = length and W = width.

Statistical analysis

The two-tailed Student's *t*-test was used to determine the statistical significance of differences in the percentage of the cell fraction evaluated by flow cytometric analysis, and in tumor size between the treatment groups. A value of $P < 0.05$ was considered to be significant. Statistical analyses were carried out using the StatView 5.0 software package (Abacus Concepts, Calabasas, CA, USA).

Results

NIH3T3-HSP105 cells acquired resistance to apoptosis induced by stressors

To elucidate the biological function of HSP105 in cancer cells, we first transfected the murine HSP105 expression vectors or an empty vector into murine embryonal fibroblast NIH3T3 cells, which are known to express smaller amounts of HSP105 than cancer cells. Subsequently, NIH3T3-mock cell lines and NIH3T3-HSP105 cell lines overexpressing HSP105 protein were established after selecting cells with G418 (Fig. 1A). There was no difference in either the morphology or the proliferative characteristics between these two cell lines cultured in DMEM supplemented with 1, 5 or 10% FCS (data not shown).

In a previous study, Hatayama *et al.* reported that rat neuronal cells overexpresing murine HSP105 were able to avoid undergoing apoptosis induced by several kinds of stressors.[8] We therefore examined the anti-apoptotic effects of HSP105 overexpression in NIH3T3-HSP105 cells. We exposed NIH3T3-mock cells and NIH3T3-HSP105 cells to heat shock at 45°C for 90 min and then detected annexin V-positive early apoptotic cells by flow cytometric analysis. The proportion of annexin V-positive NIH3T3-HSP105 cells was smaller than that of NIH3T3-mock cells ($P < 0.01$) (Fig. 1B).

We further treated these two cell lines with 200 ng/mL doxorubicin, which is known to be an inducer of apoptosis. After incubating NIH3T3-mock cells with doxorubicin for 12 h, annexin V-positive cells were detected by flow cytometric analysis. The number of annexin V-positive cells increased gradually thereafter, and almost all cells were stained with annexin V by 24 h after the treatment. However, even after 36 h incubation of cells with doxorubicin, only a small fraction (<18%) of NIH3T3-HSP105 cells were stained with annexin V. The difference in the number of annexin V-positive cells at 48 h after treatment was statistically significant ($P < 0.001$) between NIH3T3-mock and NIH3T3-HSP105 (Fig. 1C).

We next examined the DNA fragmentation of those two cell lines, which is observed during the late phase of apoptosis by staining with PI. The percentage of NIH3T3-HSP105 cells exhibiting DNA fragmentation was less than that of NIH3T3-mock cells, and the difference was statistically significant at both 36 h ($P < 0.001$) and 48 h ($P < 0.0001$) after doxorubicin treatment (Fig. 1D). These data suggest that HSP105 has an anti-apoptotic effect against apoptosis induced by heat shock and doxorubicin.

HSP105 siRNA induced various human cancer cell lines to undergo apoptosis

We previously reported that HSP105 protein is overexpressed in various human tumors and in the testis of normal adult men, but not in colon adenoma, by immunohistochemical analysis.[15] We thus examined the function of HSP105 protein in cancer cells by downregulating *HSP105* gene expression with siRNA. We used two human colon cancer cell lines, HCT116 and SW620, in which the expression of HSP105 mRNA was significantly elevated in comparison to that in normal human colon epithelium (Fig. 2A). At approximately 24 h after transfection, the adherent HCT116 cells treated with HSP105 siRNA started peeling off, and almost all of the cells had peeled off and were observed as dying cells at 48 h after transfection. In contrast, most of the HCT116 cells treated with luciferase siRNA proliferated normally (Fig. 2B). In a western blot analysis of HCT116 cells, the expression of HSP105 protein was markedly suppressed after treatment with two different HSP105-specific siRNA (HSP105-siRNA and HSP105-siRNA-2), and those cells were significantly stained with FITC–annexin V based on flow cytometric analysis (Fig. 2B,C).

Similarly, in SW620 cells after treatment with HSP105-siRNA, the expression of HSP105 protein was suppressed and a significant number of annexin V-positive cells were detected in proportion to the concentration of siRNA administered to the SW620 cells. The siRNA effect was more notable at 24 h than at 48 h after siRNA treatment in SW620 (Fig. 2C). This finding may be associated with the fact that the expression of HSP105 in SW620 was much higher than any of the other cancer cell lines tested (Fig. 3A). In addition, in other cancer cell lines, including the human hepatoma cell line SK-Hep1, human pancreatic cancer cell line PK8, and two human gastric cancer cell lines KATO-3 and MKN28, HSP105 protein expression was suppressed and all of these cell lines underwent apoptosis at 48 h after transfection of HSP105 siRNA (Fig. 2D). These data indicate that the suppression of HSP105 protein expression by siRNA can thus induce human cancer cells originating from various tissues to undergo apoptosis.

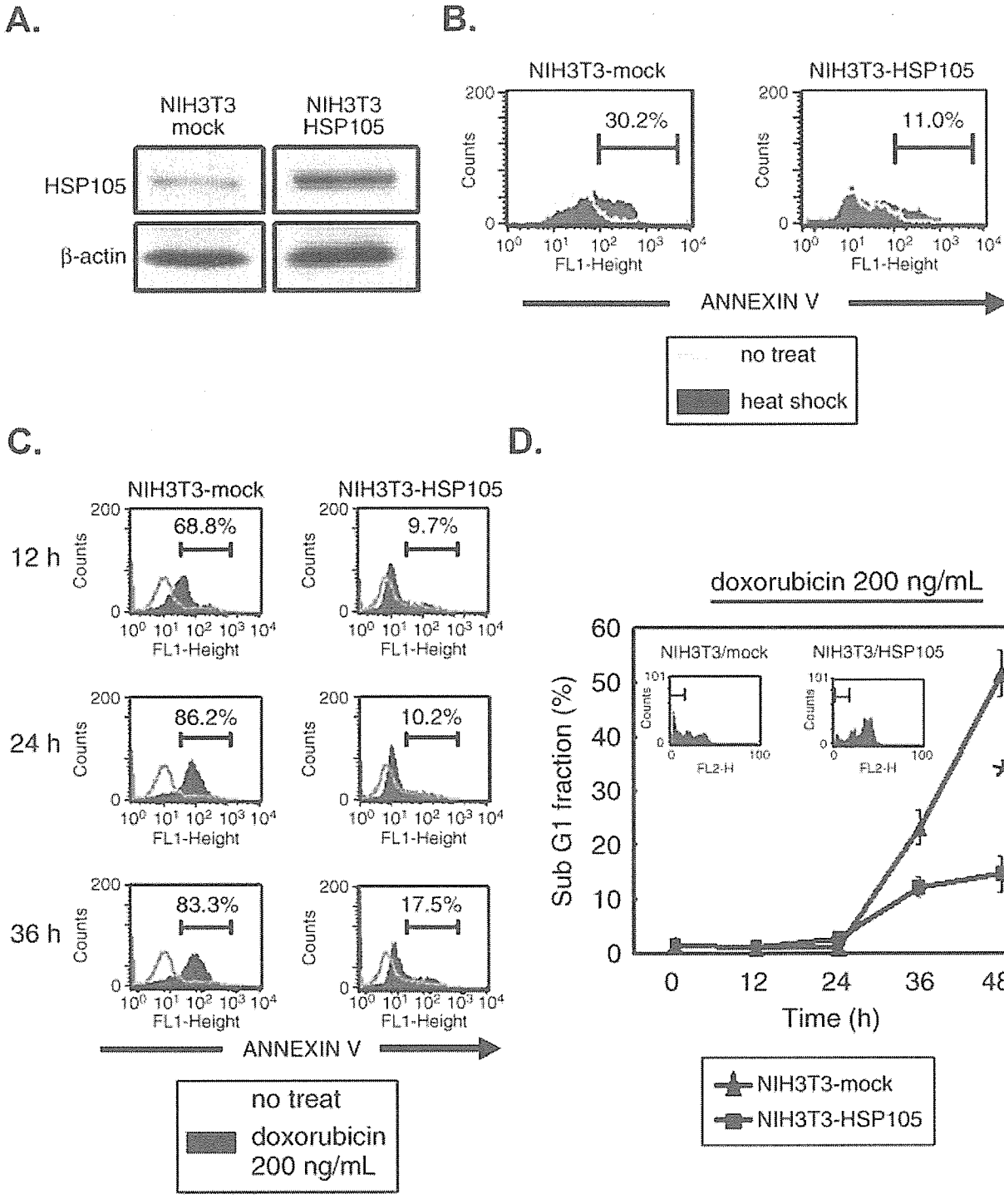

Fig. 1. Anti-apoptotic effect of HSP105 overexpression on NIH3T3 cells. (A) Western blot analysis of HSP105 expressed in NIH3T3 cells transfected with pCAGGS-IRES-neo-R or pCAGGS-IRES-neo-R-HSP105. β-Actin is shown as a control for the equal loading of protein. (B–D) Flow cytometric analyses of apoptotic cells. NIH3T3-mock cells and NIH3T3-HSP105 cells were treated at 45°C for 90 min (B) or with 200 ng/mL doxorubicin (C,D). To detect early apoptotic cells, the cells were harvested at the times indicated, stained with fluorescein-isothiocyanate–annexin V and analyzed by flow cytometry (C,D). These data are representative of at least three independent experiments. Percentages shown in the panel indicate percentage of annexin V-positive cells in heat-treated cells (B) and doxorubicin-treated cells (C). (D) Detection of DNA fragmentation by propidium iodide staining. The percentage of sub-G_1 fractions at the times indicated is shown, and the representative data of flow cytometric analysis at 48 h is shown in the panel. Data are mean ± SD ($n = 3$). The asterisk indicates that the difference in the percentages of the sub-G_1 fractions is statistically significant between the two values indicated by lines ($P < 0.001$).

doi: 10.1111/j.1349-7006.2006.00217.x

HSP105 siRNA did not induce human fibroblasts to undergo apoptosis

HSP105 is a stress-induced protein that is usually expressed ubiquitously at low levels, except in the brain and testis. To investigate the effect of HSP105 siRNA on normal cells, we applied HSP105 siRNA to human fibroblasts, Turu and Mori, generated from healthy donors. In western blot analysis, the level of HSP105 protein expressed in the Turu and Mori cells was lower than in the cancer cell lines (Fig. 3A). The expression of HSP105 protein was suppressed with HSP105 siRNA treatment, as shown in Fig. 3B,C, and the shape of fibroblast cells changed from fusiform to a round shape, but those cells were not induced to undergo apoptosis. Approximately 10 days after HSP105 siRNA transfection, both the expression of HSP105 protein and cell shape were restored (data not shown). These results indicate that the suppressive effect of HSP105 siRNA on the HSP105 expression is transient and reversible, and that the marked reduction of HSP105 protein does not have any harmful effect on normal fibroblasts under non-stressed conditions.

HSP105 siRNA treatment suppressed the growth of tumors overexpressing HSP105 *in vivo*

Small interfering RNA treatment using liposomes suppresses tumor growth *in vivo*.[21,23] To elucidate the effects of HSP105 siRNA on growing tumors *in vivo*, we injected either HSP105 siRNA or irrelevant siRNA locally into 5–7 mm KATO-3 tumors transplanted in NOD SCID mice every 3 days. As shown in Fig. 4, HSP105 siRNA suppressed tumor growth significantly in comparison to the irrelevant siRNA ($P < 0.01$). On day 15 after the first injection of HSP105 siRNA into tumors, the volumes of the tumors remained almost the same as those on day 0. During this observation period, neither abnormal behaviors nor neurological abnormalities were observed in these HSP105 siRNA-treated mice, and the expression of HSP105 protein in the brain was not suppressed by immunohistochemical analysis (data not shown).

Synergistic effects of siRNA and doxorubicin or heat shock on the *in vitro* induction of apoptosis in tumor cells

For the treatment of cancer patients with advanced, unresectable or recurrent focus, chemotherapy, radiation and other therapies are applied singly or in combination. To investigate the feasibility of combined treatment of tumor cells with HSP105 siRNA and other treatments, we treated HCT116 cells with HSP105 siRNA and either heat stress or doxorubicin. At 12 h after siRNA transfection into HCT116 cells, we added 200 ng/mL doxorubicin or treated the cells with heat shock at 45°C for 30 min, and detected the presence of apoptotic cells by staining with annexin V after 36 or 24 h incubation, respectively. As shown in Fig. 5, both combined treatments synergistically induced HCT116 cells to undergo apoptosis in comparison with the single treatment ($P < 0.001$).

Apoptosis induced by HSP105 siRNA was dependent on the caspase cascade but not on the p53 pathway

To investigate whether caspases are involved in apoptosis induced with siRNA, we examined PARP cleavage by western blot analysis using HCT116 cells with wild-type p53. PARP, a nuclear enzyme involved in DNA repair, is a well-known substrate for caspase-3, and is cleaved from a 112-kDa protein to an 85-kDa protein by the activation of caspase-3. As shown in Fig. 6A, cleavage of PARP was observed in those cells transfected with HSP105 siRNA. Moreover, this cleavage was completely inhibited by adding a pan-caspase inhibitor, Z-VAD-FMK. As a result, the apoptosis induced by HSP105 siRNA was also inhibited by Z-VAD-FMK.

We next examined whether the p53 tumor suppressor protein is involved in HSP105 siRNA-induced apoptosis. The p53 protein is located upstream of the caspase cascade and is associated with heat shock proteins such as HSP70 and HSP90.[24] As shown in Fig. 6C, the HSP105 and p53 proteins were coimmunoprecipitated with anti-HSP105 antibodies and the DO-1 in non-treated HCT116 cells. These results indicate that a proportion of HSP105 protein is bound to p53 protein in non-treated HCT116 cells. Furthermore, the expression of p53 protein decreased with HSP105 siRNA treatment at the post-transcriptional level (the mRNA expression of p53 was not suppressed), and p53 protein was not phosphorylated at serine 15 or serine 46 by this treatment (Fig. 6D,E). Furthermore, to confirm the suppression of p53 transcriptional activity, the mRNA expression of Bax, NOXA and PUMA, which are the transcriptional targets of p53-mediated apoptosis, were assessed by RT-PCR and found to be suppressed (Fig. 6E). These data suggest that HSP105 protein is thus associated with wild-type p53 protein in HCT116 cells under non-stress conditions, and HSP105 siRNA-induced apoptosis is dependent on caspases but independent of the p53-mediated apoptosis pathway.

Discussion

In the present study, we obtained the following results: (1) HSP105 protein protects tumor cells from apoptosis; (2) constitutive overexpression of HSP105 protein is essential for the survival of various kinds of cancer cells; and (3) apoptosis induced with HSP105 siRNA treatment is dependent on caspases but not p53.

Recent studies, including ours, have shown that HSP105 is overexpressed in various human tumors and that HSP105 is thus speculated to be involved in both tumorigenesis and protection of cells from apoptosis.[8,14,15] Our data obtained using NIH3T3-HSP105 cells are consistent with the findings of a recent study on neuronal PC12 cells in which the overexpression of HSP105 did not affect the growth rate of PC12 cells, but the apoptosis induced by stressors was inhibited in those cells.[8] These data indicate that HSP105 is involved in tumorigenesis through protection of cells against apoptosis.

Among the heat shock proteins, HSP70 is well characterized and HSP105 shares functional properties with HSP70. HSP70 also inhibits apoptosis induced by various stimuli.[25–27] Furthermore, HSP70 is also overexpressed in human breast cancer.[28–31] One difference in function between HSP70 and HSP105 is that HSP105 has an increased capacity to bind to denatured polypeptides in comparison to HSP70.[32] In addition, HSP105 suppresses the aggregation of denatured proteins under stress conditions in the presence of ADP, whereas HSP70 suppresses it in the presence of ATP.[7] In breast cancer cell lines, inhibition of HSP70 expression by antisense cDNA causes those cells to undergo apoptosis, and this action is

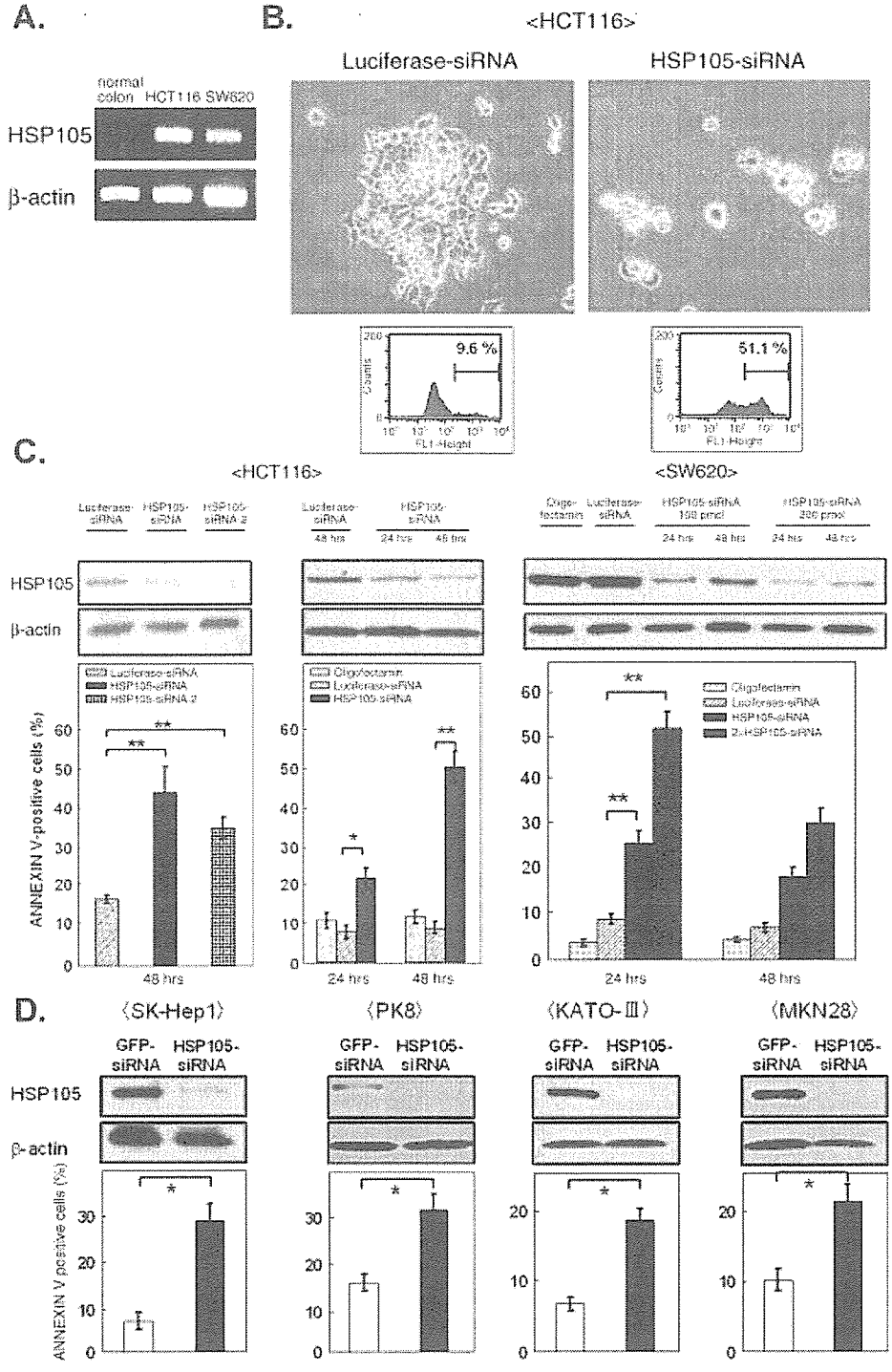

Fig. 2. Small interfering RNA (siRNA)-mediated inhibition of HSP105 expression enhanced the apoptotic cell death of human cancer cell lines. (A) Reverse transcription–polymerase chain reaction analysis of HSP105 mRNA expression in normal human colon epithelium, and in human cancer cell lines HCT116 and SW620. (B) Light microscopic pictures of HCT116 cells introduced with or without siRNA and representative flow cytometric analysis data of apoptotic cells stained with annexin V at 48 h after transfection. (C,D) Western blot analysis of HSP105 protein expression and flow cytometric analysis of apoptotic cells. HCT116 cells and SW620 cells were treated with oligofectamine, control siRNA, HSP105-siRNA (100 nM or 200 nM) or HSP105-siRNA-2 (B,C). (C) For western blot analysis, the cells were lysed at 24 or 48 h after transfection and analyzed. β-Actin is shown as a quantitative control. For flow cytometric analysis, cells were harvested at 24 or 48 h after transfection and then stained with fluorescein-isothiocyanate–annexin V and analyzed by flow cytometry. (D) Western blot analysis of HSP105 protein expression in cancer cell lines including SK-Hep1, PK8, KATO-3 and MKN28, and flow cytometric analysis of apoptotic cells at 48 h after transfection with 100 nM green fluorescent protein siRNA (□) or HSP105 siRNA (■). Data are the mean of three independent experiments ± SD. The asterisks indicate that the differences in the percentages of annexin V-positive cells are statistically significant between the two values indicated by lines (*$P < 0.01$; **$P < 0.001$).

doi: 10.1111/j.1349-7006.2006.00217.x